FILE COPY
NO. 1-W

file as NACA-TN-841

CASE FILE
COPY

TECHNICAL NOTES

NATIONAL ADVISORY COMMITTEE FOR AERONAUTICS

No. 841

THE PHOTOVISCOUS PROPERTIES OF FLUIDS

By R. Weller, D. J. Middlehurst, and R. Steiner
State College of Washington

FILE COPY
To be returned to
the files of the National
Advisory Committee
for Aeronautics
Washington, D. C.

Washington
February 1942

Reproduced by
NATIONAL TECHNICAL
INFORMATION SERVICE
Springfield, Va. 22151

4p

NATIONAL ADVISORY COMMITTEE FOR AERONAUTICS

TECHNICAL NOTE NO. 841

THE PHOTOVISCOUS PROPERTIES OF FLUIDS

By R. Weller, D. J. Middlehurst, and R. Steiner

SUMMARY

A method has been developed that permits the extension of the methods of photoelasticity to include the measurement of velocity distribution in a moving fluid. The method is based on the fact that viscous shear in certain liquids gives rise to double refraction, which may be linearly related to the shear stresses. The optical sensitivity of numerous liquids has been measured in suitable calibrating apparatus. Subsequently a closed circulating system was constructed and the velocity distribution was studied around certain simple shapes. The results indicate that the method may be profitably used to investigate problems in fluid flow not easily attacked in other ways.

INTRODUCTION

The development of double refraction in a liquid as a result of viscous shear will be termed "photoviscosity." The degree to which a liquid develops photoviscosity for a given rate of shear will be called its photoviscous sensitivity. This property has been studied from time to time since it was reported by Maxwell (reference 1) in 1874 although this report does not seem to have been the first record of its existence. Most of these studies have been concerned with the measurement of photoviscous sensitivity for a given group of liquids, and a literature of the effect has been built up. A large number of references on the subject are included in the bibliography at the end of this report. A very complete bibliography on the subject of photoelasticity is included in reference 2. A few of the observers have attempted to explain the effect in terms of assumed optical and mechanical anisotropies present in the mediums. Raman and Krischnan (reference 3) in 1928 published the most elaborate of the theories in this direction. The first attempts to apply the phenomenon to the solution of engineering problems seem to have

been reported by Sadron and Alcock (references 4 and 5).

A great number of organic compounds having unusual optical properties have been developed within recent years. It seemed probable that some of these might have a higher photoviscous sensitivity than the liquids previously investigated. For example, whereas cellulose nitrate 10 years ago was the most satisfactory material for photoelastic analysis of solid models, the development of the phenol-formaldehyde and similar plastics made possible a new and improved photoelastic technique. The present paper covers an investigation of several of these newer compounds as well as certain other materials not previously reported. The investigation was undertaken primarily to discover a suitable liquid for optical fluid-flow determinations and not for the purpose of accurately measuring the photoviscous sensitivity of a large number of liquids. The apparatus and the method employed were such as to yield very little data regarding materials of low sensitivity, which were discarded without much attention. Emphasis was laid on the convenient measurement of large effects.

The assistance of the following organizations is gratefully acknowledged in providing materials for this work and information concerning these materials: Eastman Kodak Company, Bakelite Corporation, E. I. duPont de Nemours & Company, Monsanto Chemical Company, The B. F. Goodrich Company, and Research Foundation of the Armour Institute of Technology.

PHOTOVISCOSITY

The phenomenon of photoviscosity involves the development of directional optical properties in a liquid in which a velocity gradient is present. Such a velocity gradient sets up stresses in the liquid as a result of viscous shear. These shearing stresses are proportional to the gradient and to the viscosity (absolute). By analogy with the photoelastic effect, a tension and a compression at right angles to each other and at 45° on either side of the shears may be substituted for these shearing stresses. (See fig. 1.) These may be taken as the "principle stress directions" in the liquid. In many liquids the directions of the minimum and maximum refraction indices are found to lie along these principal stress directions. Where these directions do not coincide, the theory will probably re-

quire rather specific assumptions as to the character of the liquid.

A liquid which develops birefringence in such a way that the index of refraction is reduced for light in which the electric vector vibrates in the direction of "principal tension" and is increased in the direction of "principal compression" is said to be positively birefringent and vice versa. Both positive and negative liquids have been observed. In some cases the sign of the birefringence reverses as the rate of shearing increases. (See reference 6.)

METHODS OF MEASUREMENT

Maxwell (reference 1) suggested that photoviscous birefringence be measured by placing the liquid between an outer stationary hollow cylinder and a concentric inner rotating cylinder. This apparatus was to be placed in a polariscope and the interference patterns were to be observed. Figure 2 shows such an arrangement schematically. Here the velocity of the liquid at a given radius R varies according to the relationship

$$V = V_1 \frac{\log_e R_2 - \log_e R}{\log_e R_2 - \log_e R_1}$$

in which V_1 is the peripheral velocity of the inner cylinder, R_1 is the radius of the inner cylinder, and R_2 the inner radius of the outer cylinder. The accompanying velocity gradient on which the optical effect depends is found by differentiation to be

$$\frac{dV}{dr} = - \frac{V_1}{R(\log_e R_2 - \log_e R_1)} = - \frac{A}{R}$$

where

$$A = \frac{V_1}{\log_e R_2 - \log_e R_1}$$

It will be observed that this gradient is not constant over the gap between the two cylinders and therefore a reference point must be chosen in the gap at which measurements are to be made. It is convenient to measure the velocity gradi-

ent at the midpoint of the gap between the two cylinders, this point being very close to the average value.

The method by which the calibration is made depends on the sensitivity of the liquid being tested. One way is simply to count the fringes that pass the center of the gap as the speed of the inner cylinder is slowly increased. If the order of interference is more than three or four, monochromatic light must be used in order to maintain sharply defined fringes. The effect is also proportional to the length of light path through the liquid; the number of fringes may be doubled by doubling the length of the path. The sensitivity of the apparatus therefore depends on this dimension.

Inasmuch as counting fringes is an inaccurate process, it is better to introduce a Babinet Soleil compensator at the point indicated in figure 2. With the polarizer and the analyzer crossed and the compensator set at zero, the field will be dark when the inner cylinder is stationary. If the inner cylinder is now rotated, light will be restored and the compensator may be employed to return the field to blackness. The amount of birefringence may then be read directly on the compensator scale. It is better to use white light because in this instance the zero-order fringe is the only one that appears black; all others are colored and confusion, therefore, does not exist as to the degree of compensation obtained.

Two types of Babinet Soleil compensators are available. If the ordinary compensator is used, a series of parallel fringes appear in the field, the center one being black when compensation is complete. If the Babinet Soliel type of compensator is used, the entire field is compensated by a constant amount, any variation over the field being due to the variation in the velocity gradient of the liquid. The Babinet Soleil type of compensator was employed in the present investigation.

When the effect is small, as it has been in all previously reported data, spectroscopic methods may be used. Here the light emerging from the polariscope is projected into a spectrometer. As the birefringence of the fluid increases, certain of the spectral colors will be restored and will be visible in the spectrometer. If additional birefringent material is introduced into the polariscope (such as a mica plate about 0.01 cm thick), there will be several dark bands in the spectral field. The motion of

these bands as the birefringence is varied is a rather sensitive test for double refraction.

The photoviscous sensitivity of a given material may be measured in terms of the Maxwell constant (reference 3). This constant is defined by the equation

$$n_2 - n_1 = M\mu \frac{dV}{ds}$$

in which n_1 is the refractive index in the direction of the principal tension, n_2 is the refractive index in the direction of compression, M is the Maxwell constant, μ is the viscosity of the liquid, and dV/ds is the velocity gradient. When the value of the Maxwell constant is computed for known liquids, it is found to contain a factor of the order of 10^{-11}, which renders it inconvenient to handle. In the present report this sensitivity is discussed in terms of (a) the fringe value and (b) the specific fringe value. The first of these values is defined as the velocity gradient that will produce a relative retardation of one wave length of light in a unit thickness of the liquid. The value of this constant will depend on the units used and on the wave length of the light selected, no significance being attached to this constant for white light. The specific fringe value is defined as the fringe value multiplied by the absolute viscosity (in poises).

CALIBRATING APPARATUS

The various types of apparatus employed by other experimenters in this field were considered and equipment of the same general nature was constructed. This apparatus is shown in figures 3 and 4 and was used to measure the photoviscous sensitivity of the liquids tested. The inner diameter of the outer fixed cylinder was 6.988 centimeters and that of the inner rotating cylinder 5.956 centimeters. The gap between the two cylinders was therefore 0.516 centimeter. The inner cylinder was 9.60 centimeters long, and a clearance of 0.05 centimeter was allowed at the top and the bottom.

The range of speed for the inner cylinder extended from approximately 100 rpm to 2000 rpm, making possible velocity gradients of from 30 centimeters per second per centimeter to 600 centimeters per second per centimeter.

A Babinet Soleil compensator was introduced between the two sheets of Polaroid in the polarizer and analyzer. Forty-five degree reflecting prisms were added to direct the light beam. Light was supplied by a 21-candle-power automobile headlight bulb; this light was diffused by a sheet of opal glass preceding the polarizer.

There are two techniques possible for the measurement of birefringence with this apparatus. Since one is using white light, the entire field will be black with the polarizer and the analyzer crossed, the liquid stationary, and the compensator set at zero. The inner cylinder can be set in motion and the double refraction neutralized with the compensator. This process involves an estimate on the part of the observer as to the degree of compensation obtained, and various observers do not always exactly agree. A second possibility involves the introduction of birefringence before the liquid is set in motion. The birefringence in this case may be obtained by varying the compensator setting until the so-called sensitive tint is obtained. This tint represents the transition of the interference color from red to blue, which takes place quite suddenly on a small motion of the compensator. When the liquid is set in motion, its birefringence may be measured by restoring the sensitive tint. Observations tend to agree more closely when this procedure is used.

The more sensitive liquids then were tested by the following method: The liquid was placed in the calibrator and readings were taken at various speeds so that a curve of double refraction against velocity gradient could be plotted. The viscosity of the liquid was approximately measured by the falling-ball method. Where densities were not available in handbooks, they were measured.

SENSITIVE MATERIALS

Previous investigators have discovered in studying photoviscous sensitivity that liquids may be divided according to two general classes of behavior. In one of these classes the amount of birefringence produced is closely proportional to the rate of shear. Liquids reported in this class include many oils such as olive oil, cotton-seed oil, sesame oil, etc. The second class of liquids contains the liquids that tend to saturate quite rapidly as the rate of shear increases, that is, the curve

in which rate of shear is plotted on the abscissa scale and sensitivity on the ordinate scale is convex upward and is nowhere a straight line. In this class belong such materials as the vanadium pentoxide sols, tobacco mosaic virus, and other suspensions that are probably long thin particles. Ordinary gelatin was investigated (reference 6) and was found to reverse the sign of its birefringence beyond a certain rate of shear so that, while it is relatively very sensitive, the relation between birefringence and rate of shear is quite complex. The variation in photoviscous sensitivity with temperature has also been studied. It is found that, in general, this sensitivity decreases with a decrease in temperature and the resulting reduction in the viscosity and in the magnitude of the shearing stresses. It is, of course, desirable, if photoviscous phenomena are to be used as the basis of engineering measurements, to have a liquid in which the rate of shear and birefringence are linearly related.

It seemed desirable first to investigate those materials related to photoelastically sensitive solids. These materials included the phenol formaldehydes, cellulose nitrate and acetate, the vinyl resins, such as vinyl acetate, polyvinyl butyral, polystyrene, etc. Many of these products are liquids in the primary stages of manufacture. Some are of the polymerizing type and the possibility existed of investigating various degrees of polymerization. Various plastic manufacturers were asked to contribute samples of materials that seemed promising. To these samples were added a group of oils and various random materials that occurred to the experimenters from time to time.

RESULTS

The results of this investigation are shown in table I and figures 5 and 6. Table I lists materials tested. The optical response is indicated in figures 5 and 6 in terms of the motion of the Babinet Soliel compensator. Approximately 540 divisions is the equivalent of 1 wave length of green light. The speed of the inner cylinder is given in revolutions per minute but may be converted to other units by considering the diameter of the cylinder, which is 5.956 centimeters. The curves show the variation in double refraction with the speed of rotation of the inner cylinder. For each liquid for which a curve was drawn, the fringe value is listed with the curve. The fringe

value is given by

$$F = 3120 \frac{\text{inner-cylinder speed, rpm}}{\text{compensator shift}}$$

None of the desirable liquids maintained a straight-line relationship between the rate of shear and the amount of double refraction as the rate of shear increased. This result is largely due to the rise in temperature accompanying viscous shear. This rise in temperature could have been prevented by the use of a water jacket on the calibrator. In many cases additional data indicate that a straight-line relationship can be maintained if the temperature is held constant. Various investigators have measured the relationship between temperature and photoviscous sensitivity and have found that it varies in a complicated way. The complexity is probably chiefly due to the relation between temperature and viscosity rather than to the relation between viscosity and optical response. It is natural to expect a reduction in optical response with a reduction in viscosity if the stress is directly involved because the stress is directly proportional to the viscosity. Refrigeration may therefore be employed in photoviscous experiments or the experiments may be held up until temperature equilibrium is established. In any event a calibration of the sensitive medium should be made at the working temperature.

In certain cases the liquids were diluted with appropriate solvents and the sensitivity was found to decrease by an amount proportional to the viscosity change for small amounts of solvent.

The liquids that are considered useful in engineering applications of photoviscosity are given in table II in order of increasing fringe value (decreasing sensitivity). Table II indicates the best fringe value for material 50 as well as the best specific fringe value. In addition, the effect of the increase in temperature as the apparatus was operated seems less for this liquid. Reduction in viscosity by the addition of diluents is easily accomplished.

TURBULENCE

When the photoviscous effects in liquids of low viscosity were observed, a new phenomenon appeared, which consisted of the development of a dark band in the center of the gap between the cylinders when the speed of the cylinders was increased above a certain amount. The appearance of the dark band was interpreted as due to the presence of turbulence in this region. The liquid between the dark band and the cylinder walls retained its birefringence, but the birefringence was not of the same order as would be expected in the absence of turbulence. As the speed was slowly increased, the point at which turbulence appeared could be determined with reasonable accuracy. Values of the order of 40 were obtained for Reynolds number at the onset of turbulence. The linear dimension was taken to be the gap between the cylinders and the velocity was taken as half the peripheral velocity of the inner cylinder. In order to establish clearly the argument that the dark band was due to turbulence, the viscosity of the fluid was changed by the addition of a diluting agent and the Reynolds number was found to be substantially constant.

It therefore appears that the methods of this report may be useful in studies of fluid flow which are not entirely laminar, the boundaries of turbulent regions being easily established.

Some of the liquids measured are far more sensitive than any previously reported* and there are a number that might be chosen for use in engineering applications. It is felt that these working mediums now make it practicable to employ the fringe-counting technique of the photoelastic method in the determination of velocity distributions in flowing fluids, whereas previously it was necessary to employ spectroscopic analysis in order to obtain results.

THE EXPERIMENTAL LIQUID TUNNEL

The limitations of the project made it necessary to construct a rather small experimental flow system and for

---

*No liquid previously reported in the literature on the subject of photoviscous sensitivity would have given a measurable indication of sensitivity with the present apparatus except gelatin.

this reason complex shapes could not be treated. The following cases will now be discussed:

(1) Flow in a rectangular channel

(2) Flow around a cylindrical obstruction in the channel

(3) Flow around a streamlined strut section in the channel

The methods applied to these cases are quite general and may be used in connection with any two-dimensional-flow system.

The apparatus consisted of a closed liquid system having a circulating pump and a test section through which observations were made. This equipment is shown schematically in figure 7. Figure 8 shows the equipment proper, and figure 9 shows a detail of the test section. The tunnel was constructed of 4-inch pipe, having a cross-sectional area of 12.7 square inches, or 82 square centimeters. Circulation in figure 7 is to be taken as clockwise, the liquid discharging directly from the test section into the pump and thence around the circuit before again entering the test section. It was thought that this type of circulation would eliminate any disturbances in the fluid due to the action of the pump, but it is now considered that these precautions were not necessary.

The pump was of the positive-displacement type made by the Kinney Manufacturing Company. It operates by the rotation of an eccentric roller against a sealing vane. The rated capacity at 600 rpm is 60 gallons per minute or 227 liters per minute. This type of pump construction results in a slightly pulsating discharge that is undesirable because the pulsations appear in the optical observations.

The pump was driven by a direct-current motor that was capable of a variation in speed up to double the rated speed of the pump. The motor was rated at 12 horsepower at 1200 rpm, but for most runs less than 1 horsepower was consumed. Pressure measurements made on opposite sides of the pump indicated that a differential of up to 0.2 kilogram per square centimeter was sufficient to circulate the fluid.

The pipe system was first placed horizontally, but the removal of air after opening the system was difficult and the vertical position was adopted. The vertical position possesses the advantage of a horizontal light beam and consequently greater ease of observation.

In order to maintain the liquid in the system at a pressure above atmospheric at all times, it became necessary to provide a standpipe, at the top of which was placed an air valve through which compressed air could be introduced. Leakage of fluid from the system was negligible but air intake at the pump packing and around joints became objectionable unless the air pressure was maintained at about 5 pounds. As will be noted later, this air tended to collect on the downstream side of certain test specimens and disturbed the flow pattern in the neighborhood.

Inasmuch as the fluid employed is an excellent solvent for many materials, it was necessary to take precautions to prevent contamination. Paint presents a hazard in this connection as does graphited packing in the pump bearings. When contamination results, it is necessary to resort to distillation because filtration is not adequate. Purification therefore results in the loss of the solute and a significant amount of solvent.

A detail of the test section is shown in figure 9. It consisted of a channel 1 inch wide and 5 inches deep, having quadrant-shaped entrance walls. The channel maintains its width for a space of about 3 inches and then slowly diverges. The observation windows on opposite sides of the section are made of $\frac{3}{4}$-inch glass cemented in place with Sauereisen cement. The various models were supported by spring-loaded pins that seated in holes drilled part way through the glass. This procedure eliminated the necessity of removing the windows when it became necessary to change models, access to the test section being obtained by removing the adjacent pipe elbow.

The glass windows exhibited a slight double refraction after drilling, which was evident as a slight lightening of the field in the neighborhood of the holes when the test fluid was at rest. The effect was not sufficient to cause appreciable distortion in the fringe patterns.

The optical arrangement, which is the conventional layout for two-dimensional photoelastic analysis, is shown schematically in figure 10. It involved a 100-watt, high-

intensity mercury vapor lamp, the light beam from which was collimated by a 10-inch-diameter condensing lens. The light passed through a polarizer consisting of a disk of Polaroid and a quarter-wave plate, each $8\frac{1}{2}$ inches in diameter. The emergent circularly polarized light then traversed the test section and was subsequently analyzed and projected into a camera. The problem of photography differs from that encountered in stress analysis in that a thicker layer of sensitive material is being observed. This fact renders difficult the use of an optical system having a large numerical aperture with the accompanying shallowness of field; for example, the best fringe photographs were taken with the system focused on the median plane of the test section. For this setting, however, the boundaries of both channel and model were blurred. When the side of the test section nearest the camera was in focus, the fringes were not clear. This condition is illustrated in figure 11. The remedy is obviously a field lens of very long focal length. Such a lens must be made to order and was not available. In the present report a compromise was adopted: in most cases the sharpness in the fringes was obtained at the expense of well-defined boundaries.

THE FLUID

As previously mentioned, the fluid employed was a solution of ethyl cellulose (Ethocel from The Dow Chemical Company) in ethylene glycol methyl ether acetate (Methyl Cellosolve Acetate from the Carbide & Carbon Chem. Corp.). In quantities such as those employed (15 gal or 45 liters) the cost approximated 50 cents per liter. An amount of the solute necessary to raise the viscosity at room temperature to about 30 poises was added. The significant properties of the fluid as actually used are as follows:

Concentration, grams per liter	60
Specific gravity	1.019
Absolute viscosity at 19° C, poises	30
Kinematic viscosity	29.4
Fringe value	1,200
Specific fringe value	36,000

The heat generated by stirring action did not noticeably increase the temperature of the fluid during operation. The room-temperature fringe value (1200) is therefore given. Because the sensitivity depends on the viscosity, it decreases rapidly with rising temperature and at 60° C is approximately one-half its value at 20° C.

A significant feature of this fluid is that it does not develop its principal axes of birefringence at 45° to the direction of flow. (See fig. 1.) For infinitesimal deformations the principal tension and principal compression directions make angles of 45° to the direction of flow. This condition would be expected because such directions lie at 45° to the direction of maximum shear, which is the direction of flow. The test fluid did not develop its principal axes of birefringence in these directions but in directions corresponding to a rotation of approximately 12° in the direction indicated by the shearing-force vectors.

The direction of tension therefore makes an angle of 33° to the direction of flow and the direction of compression makes an angle of 57° to the direction of flow. Reference to this effect will be made later in connection with some of the interference patterns.

THE RECTANGULAR CHANNEL

Measurements were first made using the test section alone. Fringe patterns of this condition are shown in figures 12 to 14. Figure 12 represents the flow at a pump speed of 165 rpm, the flow being at the rate of 62.5 liters per minute. Figures 13 and 14 were taken at the rate of 142 and 234 liters per minute, respectively. It will be observed that the fringes tend to become equally spaced a short distance down the channel. This spacing indicates a uniform rate of variation in the velocity gradient and hence a uniform acceleration of the velocity from the center of the channel to the walls, which is the well-known parabolic velocity distribution. Since the maximum velocity is 1.5 times the average velocity, it is easy to compute the sensitivity of the fluid as a check against the original calibrator data; for example,

Let W be the discharge in cubic centimeters per second

Let a be the half-width of the channel in centimeters

Let t be the channel depth in centimeters

Then the average velocity will be

$$V_{av} = W/2at$$

The maximum velocity will then be

$$V_{max} = 3W/4at$$

The equation representing the velocity distribution can be written

$$V = 3W/4at - 3Wx^2/4a^3t$$

The maximum velocity gradient will occur at the boundary where $x = a$ and is given by

$$dv/dx = -3W/2a^2t$$

The basic equation of the photoviscous effect is

$$dv/dx = CN/t$$

where C is the photoviscous sensitivity and N is the fringe order. Hence at the boundaries

$$3W/2a^2t = CN/t$$

or

$$C = 3W/2a^2N$$

For example, in figure 14 the value of W is 4860 cubic centimeters per second, the value of a is 1.27 centimeters, and the value of N appears to be approximately 3.75. As a result C has a value of 1200. A more accurate determination may be made by subjecting the negative to examination in a microphotometer, which accurately measures the position of the fringes. Such a record is shown in figure 15. Fringe positions from this record are shown in figure 16. Calculations based on this spacing indicate a value of 1180 for C.

The open channel illustrates the anomalous behavior

of the test medium with regard to the direction of polarization. If the principal axes of polarization developed within the fluid lie at 45° to the direction of flow, then no light would be expected to be transmitted if the plane polarizer and the plane analyzer are placed in corresponding positions. Figure 17 shows the fringe pattern for this case, it being evident that light is transmitted. If the polarizers are rotated so that one or the other lies at 33° to the direction of flow, however, the condition for extinction is satisfactory for a part of the flow. Figure 18 shows this situation. It is impossible to extinguish both sides of the channel at once because opposite rotations are necessary. A rotation of 12° from the 45° position in the opposite direction would have caused extinction over the other half of the channel.

THE CYLINDER

Figures 19 to 21 show the pattern resulting from the presence of a cylindrical obstruction to the flow. These photographs were taken with circularly polarized light, the rate of flow being 60.5, 91, and 147 liters per minute, respectively. The compromise between sharp fringes and sharp boundaries is here quite evident, sharp boundaries having been sacrificed to obtain sharp fringes.

Figure 22 shows a tracing of figure 20 in which the fringe order is indicated. It will be observed that a zero fringe occurs at five points within the pattern. The region of highest fringe order is, of course, that where the viscous drag is highest; these regions are naturally found on the sides of the cylinder and on the walls opposite the cylinder. It is interesting to notice that the effect extends over a length of the channel wall equal to approximately twice the cylinder diameter.

With this cylindrical model there was a tendency for air circulating in the system as bubbles to become attached to the trailing edge of the cylinder. The tiny black space having the shape of an arrowhead is this accretion of air. After prolonged operation at high speeds the size of the air space approached that of the model itself. The effect could have been avoided by the elimination of air from the system; but the elimination of air would have required better methods of sealing than were employed. The flow pattern around the cylinder is, of course, affected by this factor.

THE STRUT SECTION

Figures 23 to 25 show the results of substituting a section of a streamlined strut for the cylinder. The sequence of phenomena is the same as before; the rates of discharge are, however, 56.7, 89, and 182 liters per minute. As would be expected in this instance, there is less total disturbance in the flow. For a more detailed analysis of the flow figure 22 may be compared with figure 26, both of which are tracings of the fringe patterns at practically the same rate of discharge.

CALCULATION OF DRAG

The viscous drag forces on an immersed body depend upon its area, the velocity gradients over its surface, and the viscosity μ of the fluid in which the body is immersed.

$$\text{Total force} = \mu \int \text{grad } V \cos \theta \, dA$$

where $\cos \theta$ is the angle between the drag force at a particular point on the surface and the total force exerted on the shape.

A development of the boundary of the section shown in figure 23, starting at the leading edge, is shown in figure 27. The upper curve in the figure represents the fringe order, and therefore the velocity gradient, at all points. The lower curve takes into account the angle between the tangent to the boundary and the resultant drag force. The velocity gradients plotted as ordinates are the products of the gradient and $\cos \theta$. The integral around the shape gives the area under the curve and, when multiplied by the viscosity, gives the drag. The values are as follows:

Length of developed boundary, centimeters	6.04
$\int$ grad V cos θ dA, square centimeters per second	7040
Viscosity, poises	30
Drag (frictional), grams	215

The gradient is obtained simply as the product of the fringe order at each point and the fringe constant of the fluid for the thickness employed. In this case a velocity gradient of 93 centimeters per second per centimeter corresponds to a fringe order of unity.

VELOCITY CALCULATIONS

In order to determine the actual velocities present in various parts of the flow, the following procedure may be adopted. Consider figure 16, which represents the fringes in the central part of the channel for the situation of figure 14. Assume that the velocity is zero at all boundaries. Choose a path along which to integrate, such as A-B. Divide this path into sections represented by the intersections with the fringes. The velocity gradient at the boundary is 371 centimeters per second per centimeter. At the first intersection with an inner fringe, the velocity gradient becomes 279 centimeters per second per centimeter. Over the first section of the path it has an average value, therefore, of 325 centimeters per second per centimeter. If this average value is multiplied by the length of the section, the result is the change in velocity over the section. Since the velocity at the boundary is zero, this change (added to zero) gives the velocity at the end of the first section. By taking the average gradient over the second section, multiplying by the length of the section, and adding the result to the first velocity, the velocity at the end of the second section is obtained. Table III shows the values obtained in this way. A check is provided by the requirement that, when the opposite boundary is reached, the velocity must return to zero. Such integrations may be performed over any curved line in the velocity field. If a closed curve is selected that encloses the model, the result will be the circulation around the model, an important factor dynamically.

CORRECTION FACTORS

Aside from the causes of error usually associated with photoelastic experiments, there are certain effects peculiar to the use of fluid mediums of the type employed. Whether these corrections are large or small depends on the particular case under discussion. It might be

suggested, however, that one source of difficulty encountered in elastic systems is absent in fluid-flow measurements, namely, the existence of initial stresses. Whereas these initial stresses exist to a certain extent in all photoelastic models, there is no birefringence in a fluid at rest.

The anomaly in the polarization directions associated with the use of certain test fluids has already been noted. This irregularity actually introduces two types of correction. The first is the simple rotation of polarization axes, which makes it necessary to add 33° to or subtract 57° from the polarizer directions instead of the expected 45° in order to obtain the directions of flow. This rotation of axes is not a significant feature and the angles that must be used are always obvious.

The second correction arises from the same source but must be considered more carefully. With solid photoelastic models it is common to assume that the double refraction observed along any particular direction of observation arises solely from stresses lying in planes normal to this direction. The same is not true of fluids as the following example will illustrate. It is obvious that, in the channel employed in these tests, the velocity is not constant throughout the depth of the section but must become zero at the inner surface of the glass windows. Since the channel is deep as compared with its width, it is probable that variations of velocity with depth are confined to regions near the windows. Consider figure 28. Here the flow is shown from the side and an element of the fluid is shown lying in the region wherein such a velocity variation is taking place. This element deforms into the shape shown by the dotted lines in the figure and the resulting directions of polarization are indicated. Because this is a pure shear, the tension and the compression are numerically equal; and, if the tension and compression directions were at 45° to the direction of flow, their projections normal to the light beam would cancel each other. Inasmuch as the compression will actually project shorter than the tension, the projections do not cancel and a residual tension remains. This residual tension introduces an additional double refraction, which is added to that produced by the velocity gradients normal to the light direction. This effect is illustrated in figure 29, which shows the factors producing double refraction along the light beam.

This correction will alter the interpretation of the fringe patterns to a certain extent. For example, in the case of the cylinder and strut when photographed with circularly polarized light, the channel may be crossed without encountering a zero fringe. This condition is impossible for obvious reasons. If proper correction is made, the zero fringe should extend throughout the channel, dividing to pass the obstruction. This situation has been found to be true.

Several methods may be used to overcome the difficulty mentioned. Two fluid systems having the same velocities and shapes but different depths might be superimposed. If the two flows are in opposite directions the end effects will cancel, leaving a single effect due to a channel of a depth equal to the difference of the two. Probably the best solution is to utilize the scattering method of analysis. (See reference 7.) Here it seems most convenient to introduce a source of polarized light within the model. This source may be obtained by projecting a beam of unpolarized light through a slit into the test section so as to illuminate a plane section normal to the direction of observation. If this plane section were so chosen that it lay above the region in which the difficulty arises, a part of the disturbance would be removed.

CONCLUSIONS

The investigations carried out on the photoviscous properties of fluids seem to indicate that it is entirely practicable to carry over into fluid-flow studies the techniques of photoelasticity. The most satisfactory fluids found to date are solutions of certain organic materials. These materials seem to be those characterized by a complex molecular structure, which is not rigid but which is capable of considerable distortion in viscous shear. The high viscosity of the present fluids leads to abnormally low values of Reynolds number for models of reasonable size, but this difficulty can be corrected if better working mediums are found. Work is being continued in this direction.

The measurement of velocity gradients is carried out by precisely the same techniques as are employed in the photoelastic procedure. The development of polarizing axes at angles other than 45° to the direction of flow

introduces end corrections that are reduced as the aspect ratio of the test channel is increased. It is probable that these end corrections can be completely evaluated by the use of scattered-light sources.

The investigation of three-dimensional-flow problems apparently offers no special difficulties and will be studied at an early date.

State College of Washington,
Pullman, Wash., April 1941.

REFERENCES

1. Maxwell, J. C.: On Double Refraction in a Viscous Fluid in Motion. Proc. Roy. Soc., vol. 22, 1873-74, pp. 46-47.

2. Coker, E. G., and Filon, L. N. G.: A Treatise on Photo-Elasticity. The University Press, Cambridge, (England), 1931.

3. Raman, C. V., and Krischnan, K. S.: A Theory of the Birefringence Induced by Flow in Liquids. Phil. Mag., ser. 7, vol. 5, no. 30, April 1928, pp. 769-783.

4. Sadron, C. L., and Alcock, E. D.: An Optical Method for Measuring the Distribution of Velocity Gradients in a Two-Dimensional Flow. Paper presented at Aerodynamics and Hydrodynamics Summer Meeting of the A.S.M.E., June 19-21, 1934.

5. Alcock, E. D., and Sadron, C. L.: An Optical Method for Measuring the Distribution of Velocity Gradients in a Two-Dimensional Flow. Physics, vol. 6, March 1935, pp. 92-95.

6. Hill, B. V.: On Accidental Double Refraction in Liquids. Phil. Mag., vol. 48, 1899, pp. 485-498.

7. Weller, R., and Bussey, J. K.: Photoelastic Analysis of Three-Dimensional Stress Systems Using Scattered Light. T.N. No. 737, NACA, 1939.

BIBLIOGRAPHY

Fresnel, A.: Mémoire sur les couleurs développées dans des fluides homogénes par la lumière polarisée. Ann. de Chem. et Phys. (III), vol. 17, 1846, pp. 172-198.

Maxwell, J. C.: Über Doppelbrechung in einer bewegten zähen Flüssigkeit. Ann. der Phys. (II), Bd. 151, 1874, p. 154.

Kundt, A.: Über die Doppelbrechung des Lichtes in bewegten reibenden Flüssigkeiten. Ann. der Phys. (III), Bd. 13, 1881, pp. 110-133.

deMetz, G.: Über die temporäre Doppelbrechung des Lichtes in rotirenden Flüssigkeiten. Ann. der Phys. (III), Bd. 35, 1888, pp. 497-507.

Umlauf, K.: Über Doppelbrechung in rotirenden Flüssigkeiten. Ann. der Phys. (III), Bd. 45, 1892, pp. 304-315.

Schwedoff, T.: Sur une anomalie dans la réfraction double des liquides. Jour. de Phys. (III), vol. 1, 1892, pp. 49-53.

Almy, J. E.: Concerning Accidental Double Refraction in Liquids. Phil. Mag., ser. 5, vol. 44, 1897, pp. 490-503.

Reiger, R.: Innere Riebung elastischer und fester Körper. Phys. Zeitschr., vol. 2, 1900-1901, pp. 213-217.

Hill, B. V.: Note on Accidental Double Refraction in Solutions of Colloids. Phil. Mag., ser. 6, vol. 2, Nov. 1901, pp. 524-527.

Natanson, L.: Über die temporäre Doppelbrechung des Lichtes in bewegten reibenden Flüssigkeiten. Zeitschr. f. Phys. Chem., vol. 39, 1901, pp. 355-363.

Natanson, L.: On Double Refraction in Moving Viscous Liquids. Phil. Mag., ser. 6, vol. 2, Oct. 1901, pp. 342-356.

deMetz, G.: Double réfraction accidentelle des liquides mécaniquement déformés. Comptes Rendus, t. 134, June 9, 1902, pp. 1353-56.

Zaremba, S.: Note sur la double réfraction accidentelle de la lumière dans les liquides. Jour. de Phys. (IV), vol. 3, 1904, pp. 606-611; vol. 4, 1905, pp. 514-516.

Natanson, L.: Sur une particularité de la double réfraction accidentelle dans les liquides. Jour. de Phys. (IV), vol. 4, 1905, pp. 183-190.

Zakrzewski, C., and Kraft, C.: Directions principales dans les liquides biréfringents par l'effet du mouvement. Bull. Acad. Sci. (Cracovie), No. 7, July 1905, pp. 506-520.

deMetz, G.: La double réfraction accidentelle dans les liquides. Collection "Scientia", No. 26, Gautier-Villars (Paris), 1906.

Diesselhorst, H., and Freundlich, H.: Über die Doppelbrechung des Vanadin-pentoxyd Sols. Phys. Zeitschr., 16 Jahrg., Nov. 15, 1915, pp. 419-425.

Pontremoli, A.: La doppia rifrazione accidentale meccanica nei liquidi. Mem. R. Accad., Cl. Sci. Fis. Mat. e Nat., vol. 13, 1921, pp. 594-616.

Humphrey, R. H.: Demonstration of the Double Refraction Due to Motion of a Vanadium Pentoxide Solution and Some Applications. Proc. Phys. Soc. (London), vol. 35, June 1923, pp. 217-218.

Krüger, E.: Versuche zur Kenntniss der Doppelbrechung in strömenden Flüssigkeiten. Zeitschr. f. Phys. Chem., vol. 109, 1924, pp. 438-452.

Vorländer, D., and Walter, R.: Die erzwungene Doppelbrechung der amprphen Flüssigkeiten im Zusammenhange mit der molekularen Gestalt. Phys. Zeitschr. 25 Jahrg., 1924, pp. 571-573.

Vorlander, D., and Walter, R.: Die mechanisch erzwungene Doppelbrechung der amorphen Flüssigkeiten im Zusammenhange mit der molekularen Gesalt. Zeitschr. f. Phys. Chem., vol. 118, Oct. 25, 1925, pp. 1-30.

Graffi, D.: Ricerche sulla birifrangenza accidentale dei colloidi in movimento. Atti R. Accad. Naz. Lincei, ser. 6, vol. 3, June 3, 1926, pp. 28-31.

Pontremoli, A.: Circa alcune nuove ricerche sulla birifrangenza accidentale dei colloidi in movimento. Atti R. Accad. Naz. Lincei, ser. 6, vol. 3, Jan. 17, 1926, pp. 75-77.

Boeder, P.: Über Stromungsdoppelbrechung. Zeitschr. f. Phys., Bd. 75, no. 3/4, March 31, 1931, pp. 258-281.

Sadron, Charles: Sur une nouvelle methode optique d'exploration d'un champ de vitesses bidimensionel. Comptes Rendue, t. 197, Nov. 27, 1933, pp. 1293-96.

Mamul: Die Verwendung der doppelten Strahlenbrechung zur Untersuchung von Stromungen bei Flüssigkeiten. Zeitschr. f. Tech. Phys. (Leningrad), Bd. 6, 1936, pp. 2016-2028.

Sadron, C.: Sur les propriétés dynamo-optiques des liquides purs et des solution colloidales. Schweiser Archiv, vol. 3, no. 1, Jan. 1937, pp. 8-21.

TABLE I

MATERIALS TESTED FOR PHOTOVISCOUS SENSITIVITY

	Material	Sensitivity
1	Cottonseed oil	Negligible
2	Halowax oil	Neg.
3	Gelatin (Knox) 0.035 gram/cc	Good
4	Gelatin (Knox) 0.07 gram/cc	Good
5	Egg albumen	Neg.
6	Sodium silicate	Neg.
7	Gum acacia in water	Neg.
8	Oil of sassafras	Neg.
9	Oil of citronella	Neg.
10	Oil of anise	Neg.
11	Oil of eucalyptus	Neg.
12	Oil of amber	Neg.
13	Oil of pine	Neg.
14	Sperm oil	Neg.
15	Oil of cedar	Neg.
16	Oil of juniper	Neg.
17	Oil of almonds	Neg.
18	Neat's-foot oil	Neg.
19	Cod-liver oil	Neg.
20	Oil of balsam	Neg.
21	Fish oil	Neg.
22	Resin BV-10360 (Bakelite)	Cloudy
23	Resin BR-4500 (Bakelite)	Fair
24	Resin BR-48-306 (Bakelite)	Not tested
25	Resin BR-41-001 (Bakelite)	Neg.
26	Resin B-4 (XR-7428) (Bakelite)	Fair
27	Beta glucose penta-acetate	Neg.
28	Vinyl acetate polymer in monomer	Poor
29	Styrene polymer in monomer	Good
30	Resin L-1111-39 (XR-13936)	Neg.
31	Acrawax B in mineral turpentine	Neg.
32	Diglycol laurate (Glycol)	Neg.
33	Diglycol stearate in ethanol (Glycol)	Neg.
34	Abopon (Glycol)	Neg.
35	Polyvynal butyral resin in ethanol (duPont)	Fair
36	Polyvynal butyral sheeting in ethanol (duPont)	Fair
37	Vinyl acetate in ethanol (duPont)	Negligible
38	Methyl methacrylate in ethanol (duPont)	Poor
39	Polyvinyl alcohol in water (duPont)	Neg.
40	Resin R-3525 (duPont)	Neg.
41	Zein in carbitol	Neg.
42	Korolac (Goodrich)	Fair
43	Sesame oil	Neg.
44	Methyl cellosolve acetate with cellulose acetate and butyrate 160 (Kodak)	Fair
45	Methyl cellosolve acetate with cellulose acetate and butyrate 381 (Kodak)	Good
46	Methyl cellosolve acetate with cellulose acetate (Kodak)	Good
47	Dimethyl phthalate with cellulose acetate (Kodak)	Good
48	Dimethyl phthalate with cellulose acetate and butyrate 160 (Kodak)	Good
49	Dimethyl phthalate with cellulose acetate and butyrate 381 (Kodak)	Good
50	Methyl cellosolve acetate with cellulose ether (Kodak)	Good
51	Dimethyl phthalate with cellulose ether (Kodak)	Good
52	Polyvinyl acetate (Monsanto)	Good
53	Polyvinyl formal (Monsanto)	Poor
54	Polyvinyl butyral (Monsanto)	Good
55	Cellulose acetate (Monsanto)	Good
56	Cellulose nitrate (Monsanto)	Good
57	Polystyrene (Monsanto)	Good
58	Phenol-formaldehyde syrup (Monsanto)	Fair
59	Ethyl cellulose (Monsanto)	Good

TABLE II
FRINGE VALUES OF LIQUIDS USEFUL IN ENGINEERING
APPLICATIONS OF PHOTOVISCOSITY

	Material	Fringe value	Viscosity at room temperature (poises)	Specific fringe value
50	8:1 methyl cellosolve acetate with cellulose ether (Kodak)	550	67	36,800
51	16:1 dimethyl phthalate with cellulose ether (Kodak)	560	71	40,000
47	12:1 dimethyl phthalate with cellulose acetate (Kodak)	1500	79	118,000
48	14:1 dimethyl phthalate/cellulose acetate butyrate 160 (Kodak) with	2700	44	118,000
29	Polystyrene in styrene monomer (Bakelite)	4400	23.4	104,000

TABLE III
VELOCITY CALCULATIONS

Section	Average fringe order over section	Average velocity gradient (cm/sec/cm)	Length of section (cm)	Velocity change (cm/sec)	Velocity at end of section (cm/sec)
1	3.5	325	0.336	109	109
2	2.5	232	.336	77.9	186.9
3	1.5	139.5	.306	42.7	229.6
4	.5	46.5	.336	15.6	245.2
5	.5	-46.5	.336	-15.6	229.6
6	1.5	-139.5	.354	-49.4	180.2
7	2.5	-232	.346	-80.3	99.9
8	3.25	-302	.188	-56.7	43.2

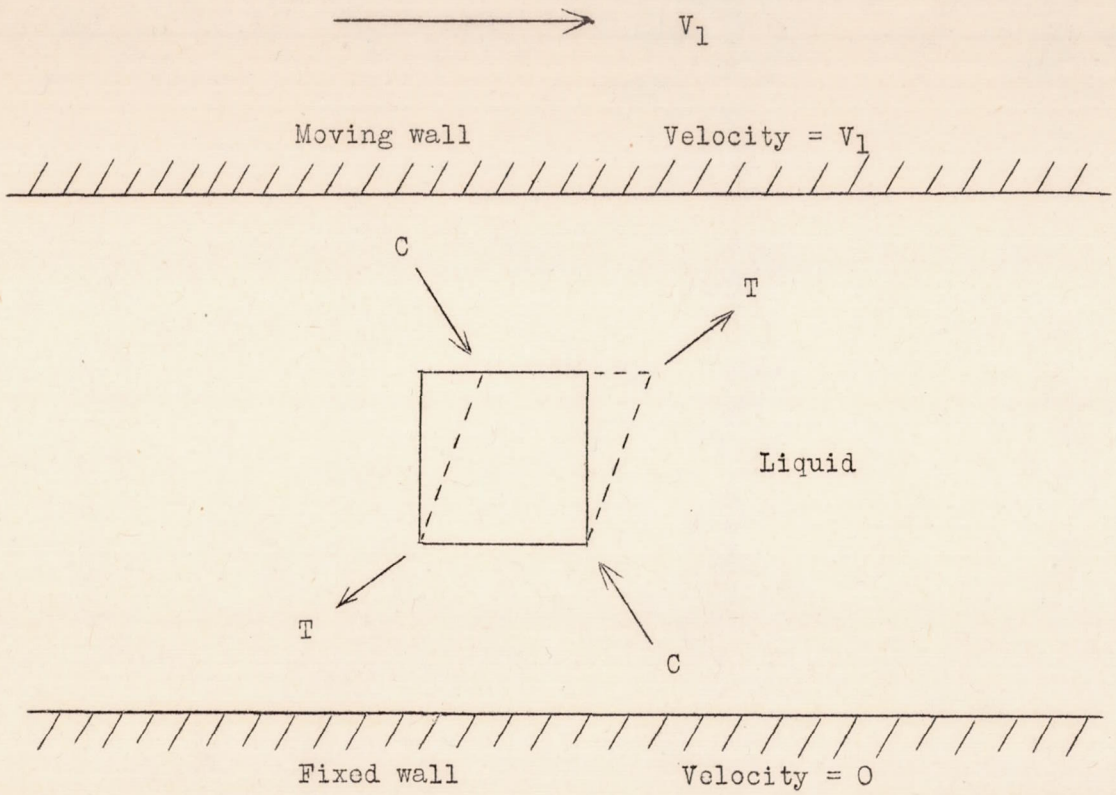

Figure 1.- Forces in a shearing liquid. An element such as the solid square deforms with time into the dotted figure.

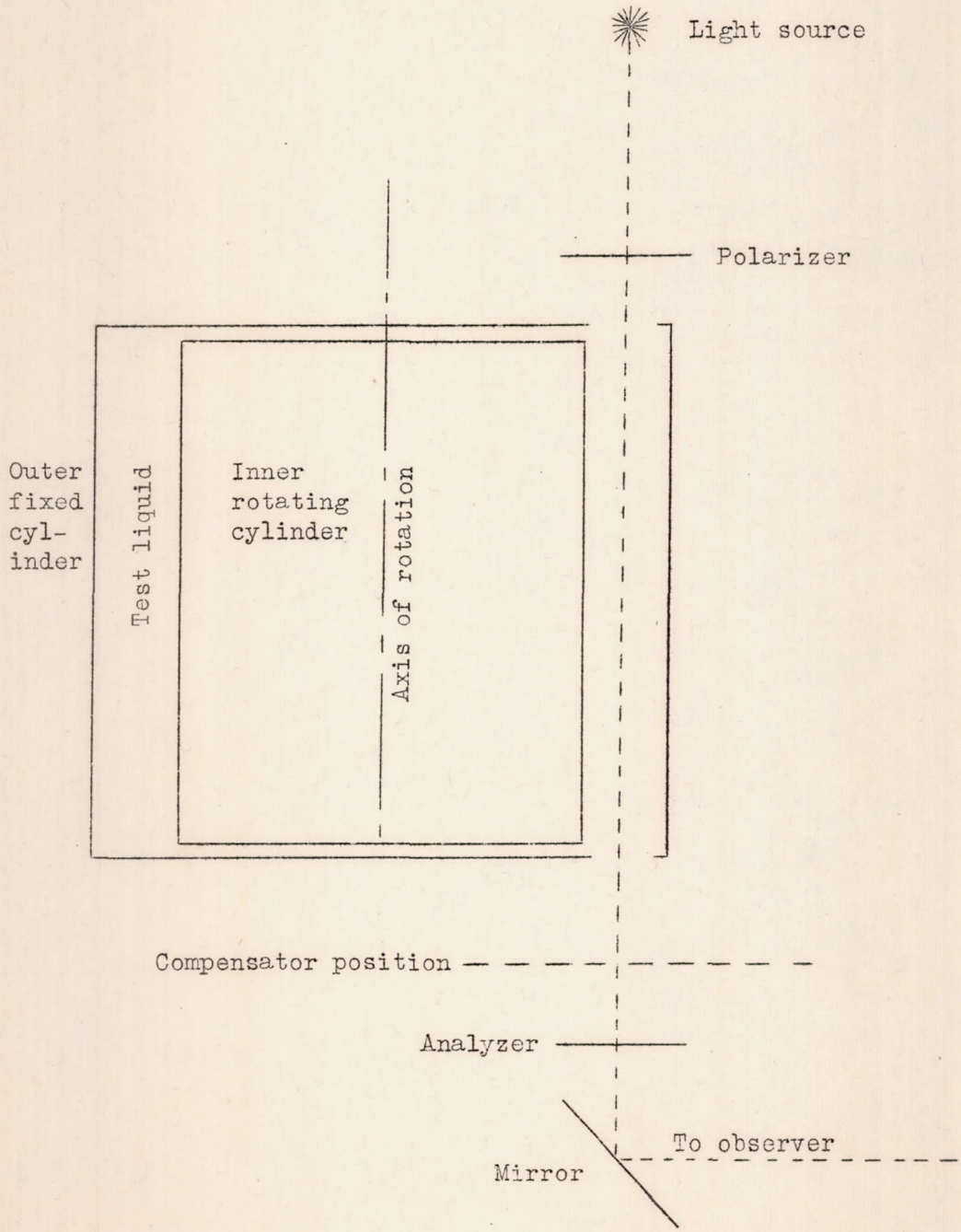

Figure 2.- Device for measuring photoviscous birefringence. Windows in the outer cylinder permit the light to pass through.

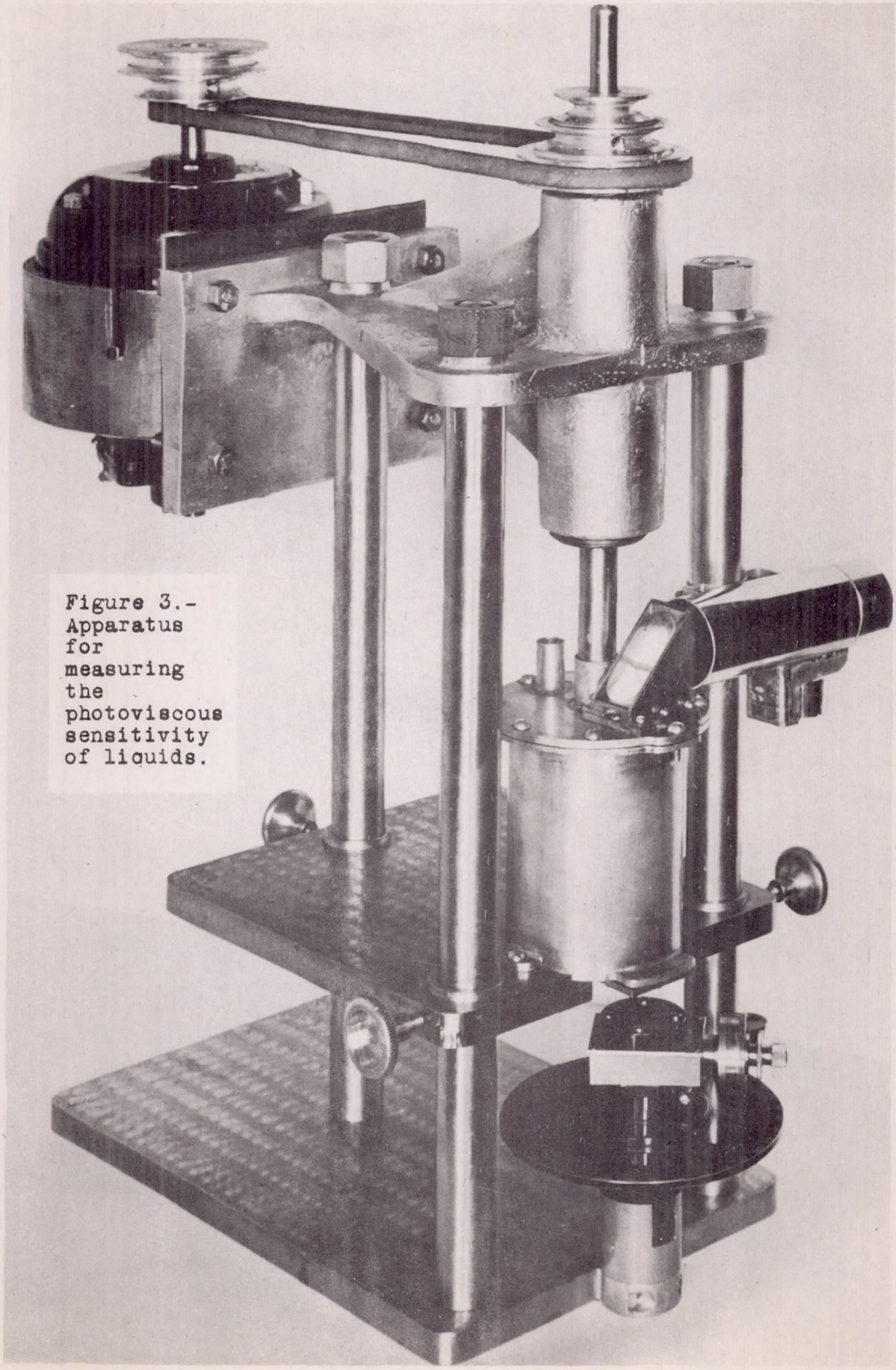

Figure 3.- Apparatus for measuring the photoviscous sensitivity of liquids.

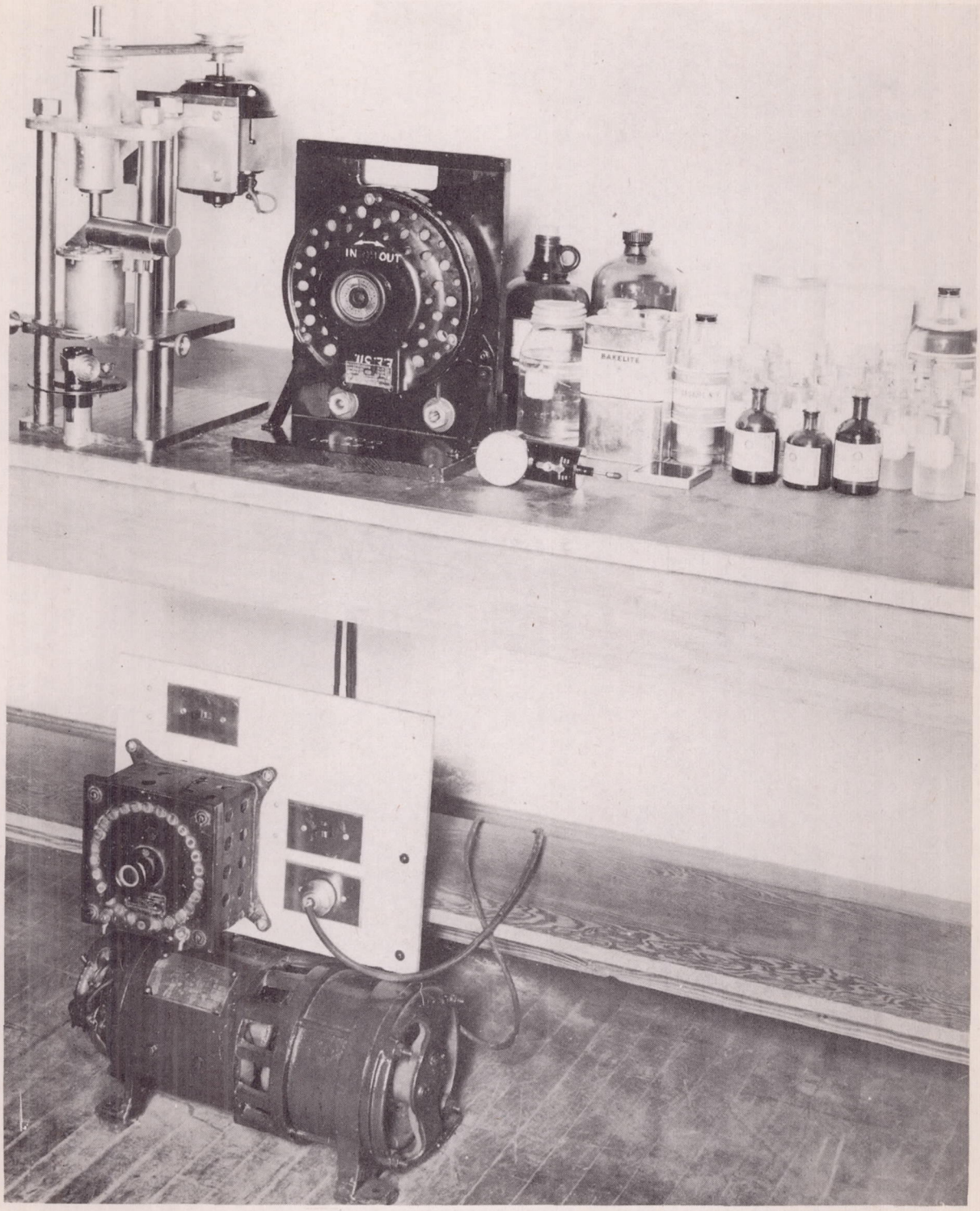

Figure 4.- Apparatus for measuring the photoviscous sensitivity of liquids and liquids tested.

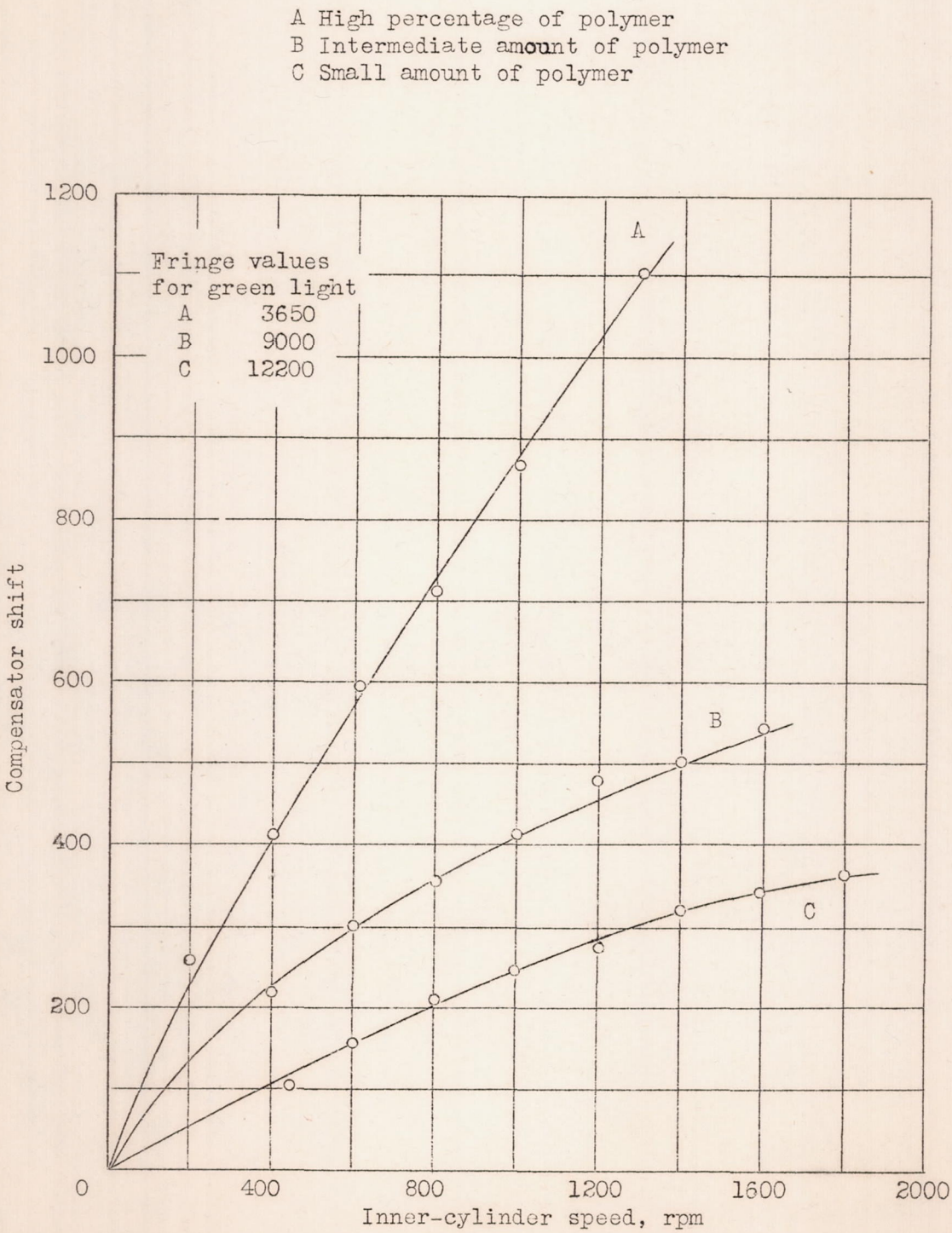

Figure 5.- Photoviscous sensitivity of polystyrene.

A Methyl cellosolve acetate cellulose ether
B Dimethyl phthalate cellulose ether
C Dimethyl phthalate cellulose acetate
D Dimethyl phthalate cellulose acetate butyrate 160
E Dimethyl phthalate cellulose acetate butyrate 160

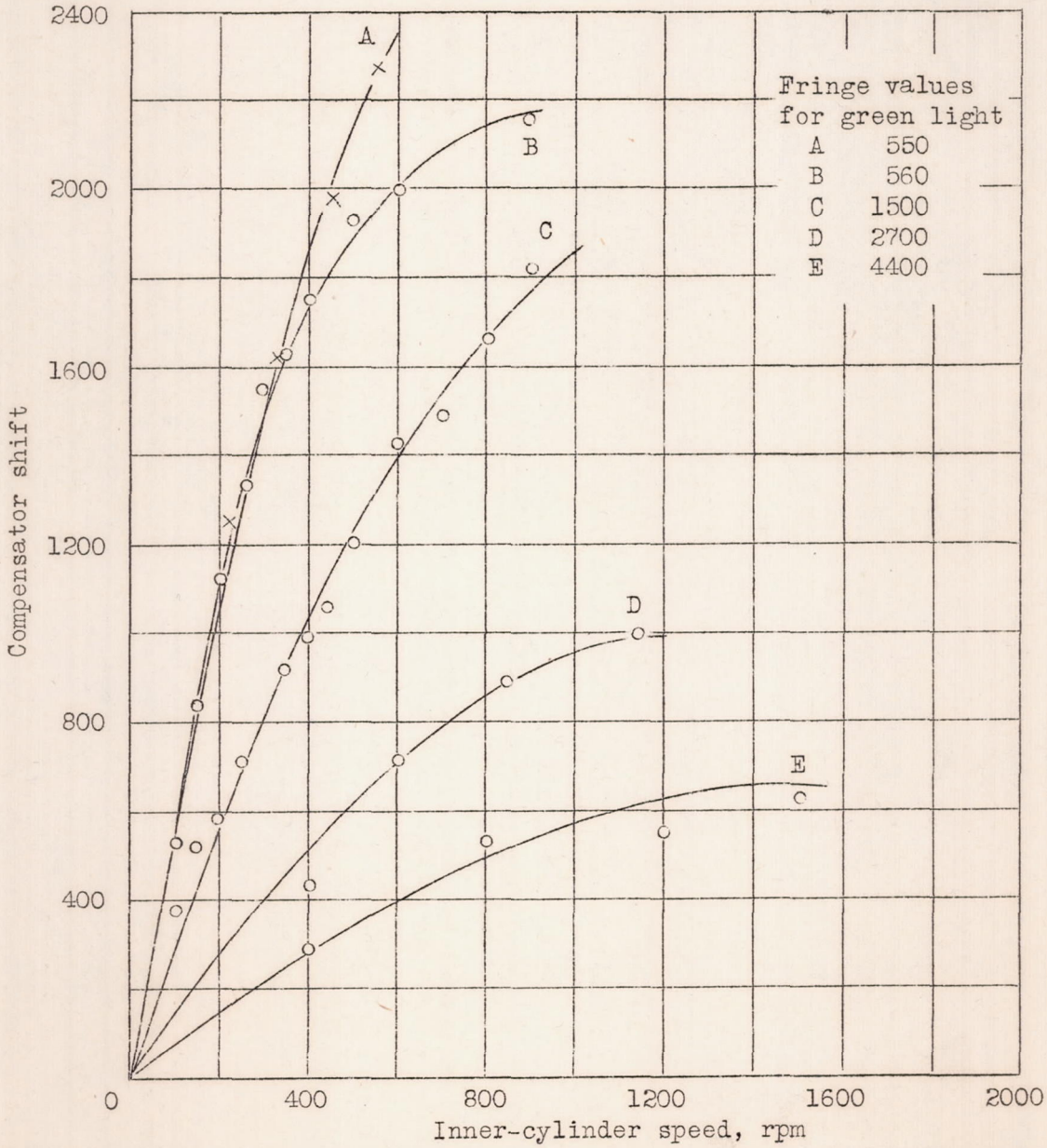

Figure 6.- Photoviscous sensitivity of materials related to photoelastically sensitive solids.

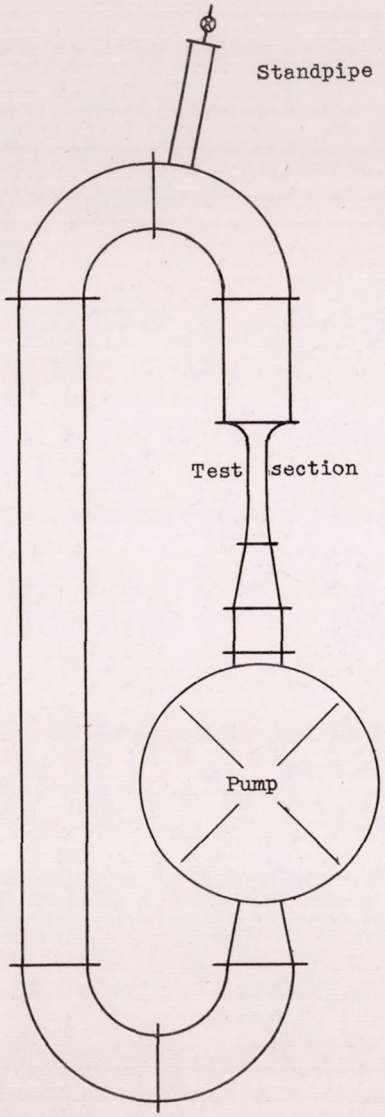

Figure 7.- Schematic diagram of photoviscous test equipment. Circulation of the fluid is clockwise.

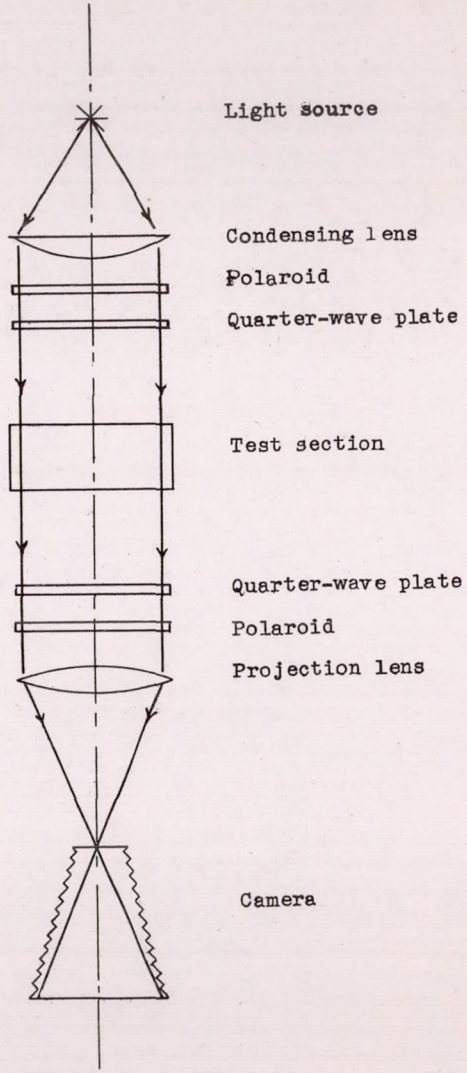

Figure 10.- Schematic diagram of the optical system.

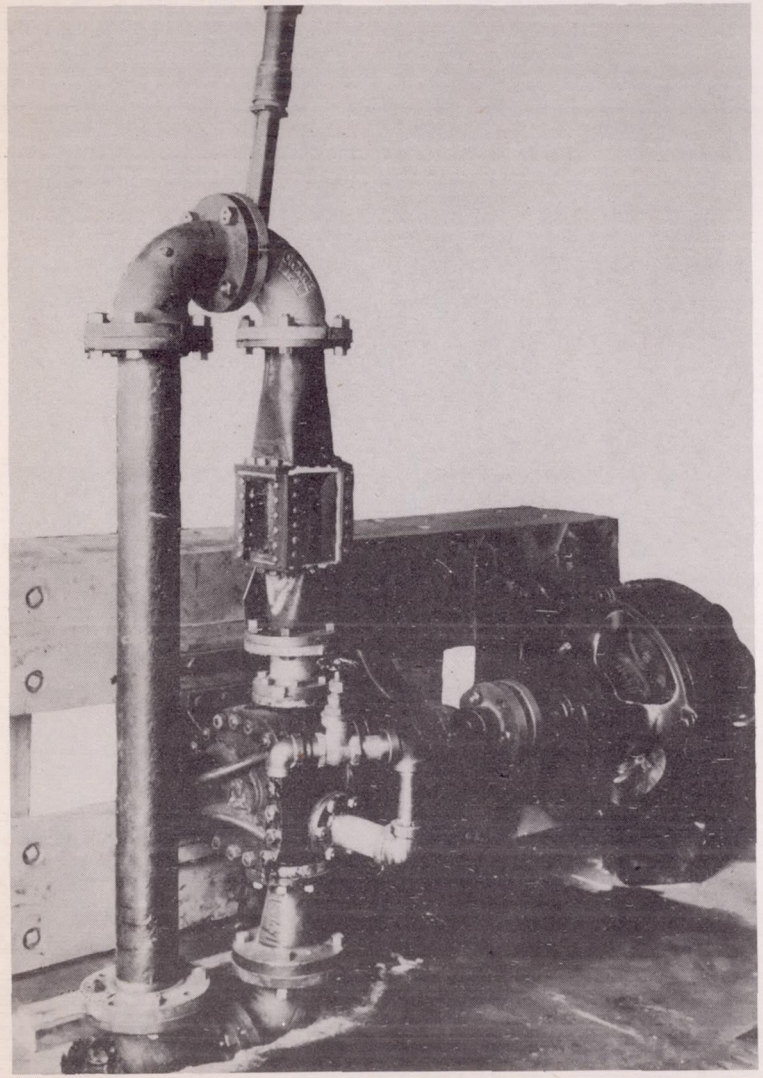

Figure 8.- General view of apparatus.

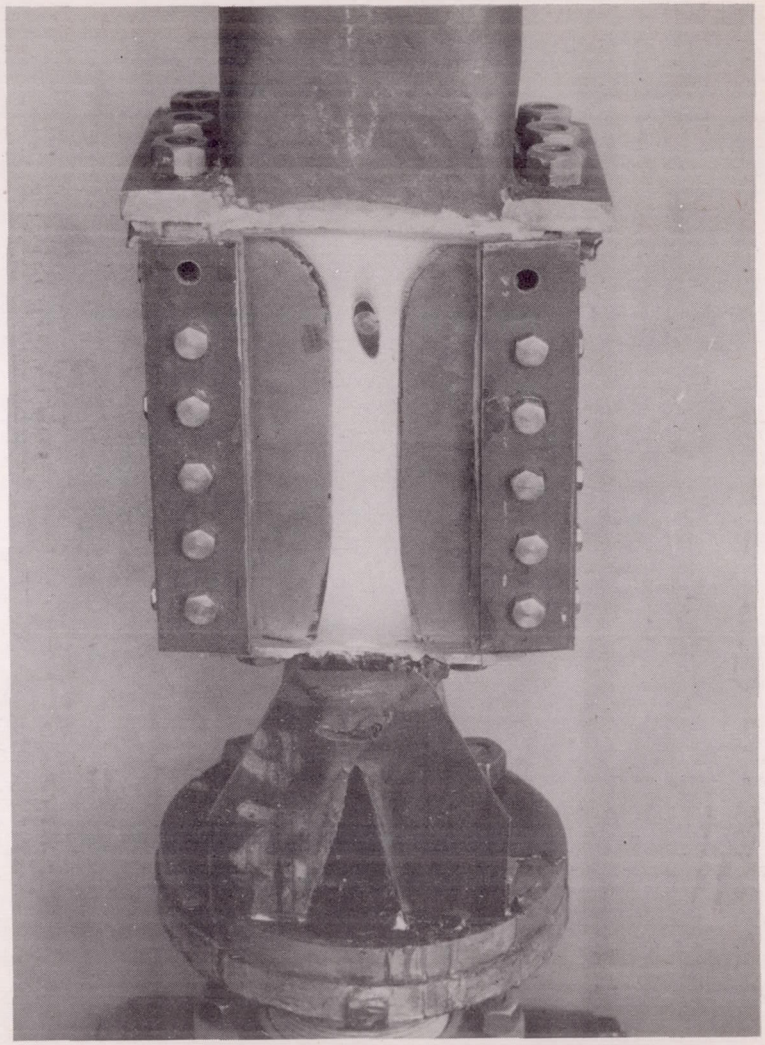

Figure 9.- View of test section in which models were placed, the strut model is in the channel.

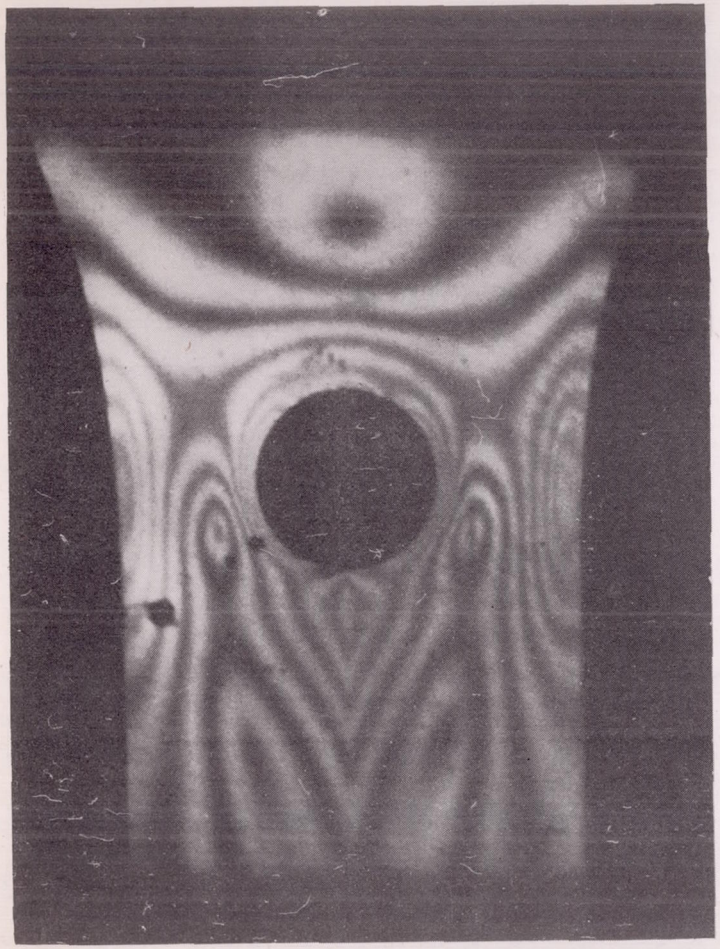

Figure 11.- Fringe photograph taken with the camera focused on the near side of the test section showing blurred fringe pattern.

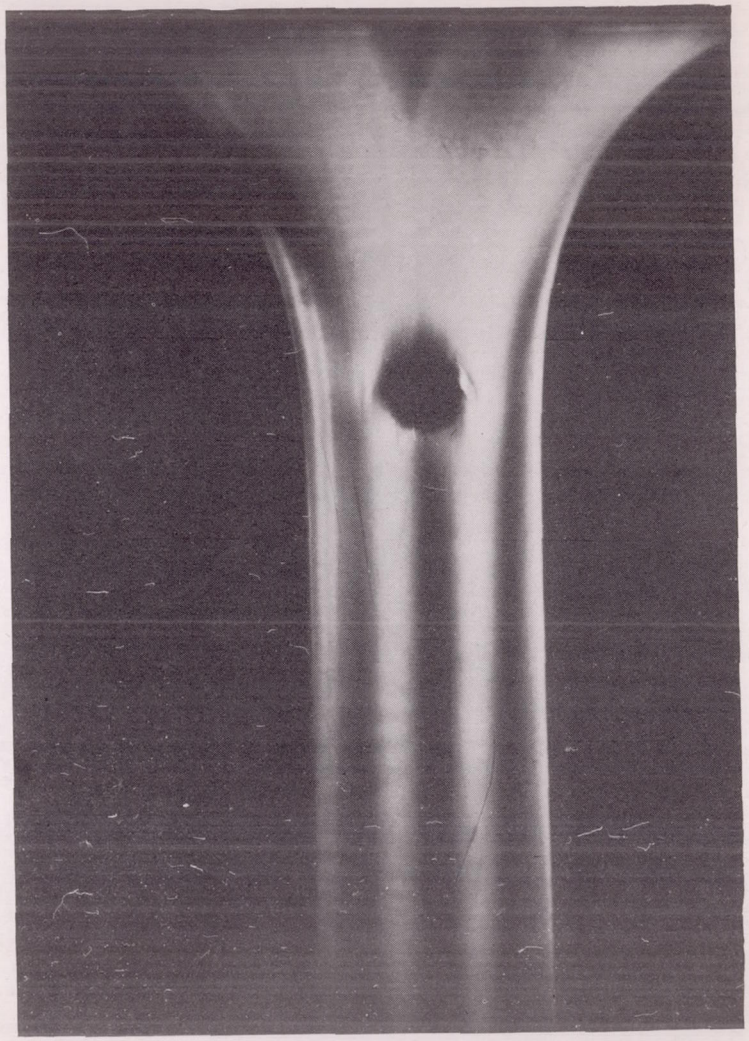

Figure 12.- Flow pattern in the unobstructed channel. Discharge rate, 62.5 liters per minute.

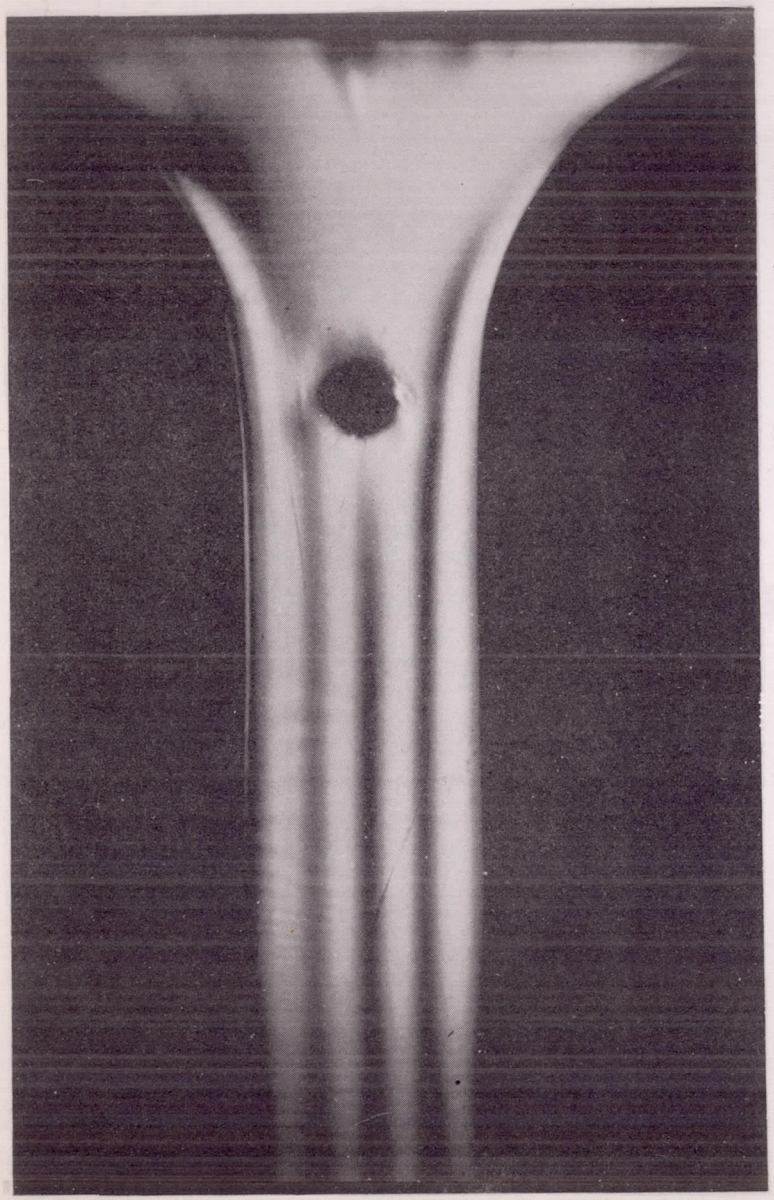

Figure 13.- Flow pattern in the unobstructed channel. Discharge rate, 142 liters per minute.

←

Figure 14.- Flow pattern in the unobstructed channel. Discharge rate, 234 liters per minute.

→

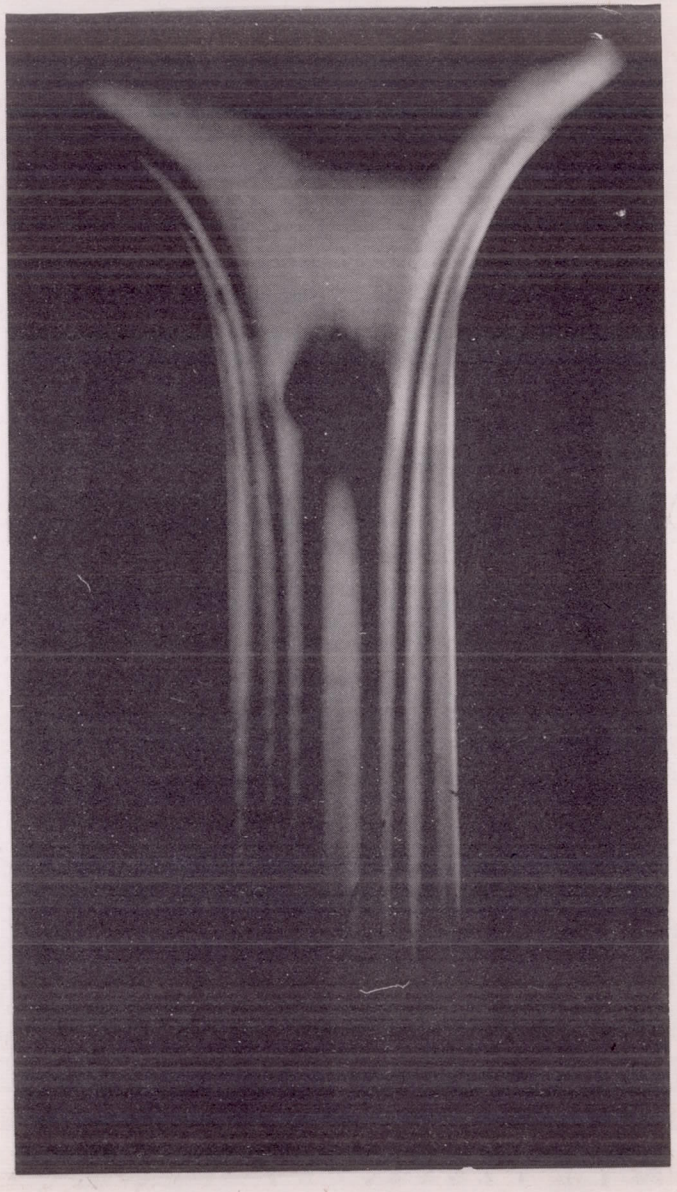

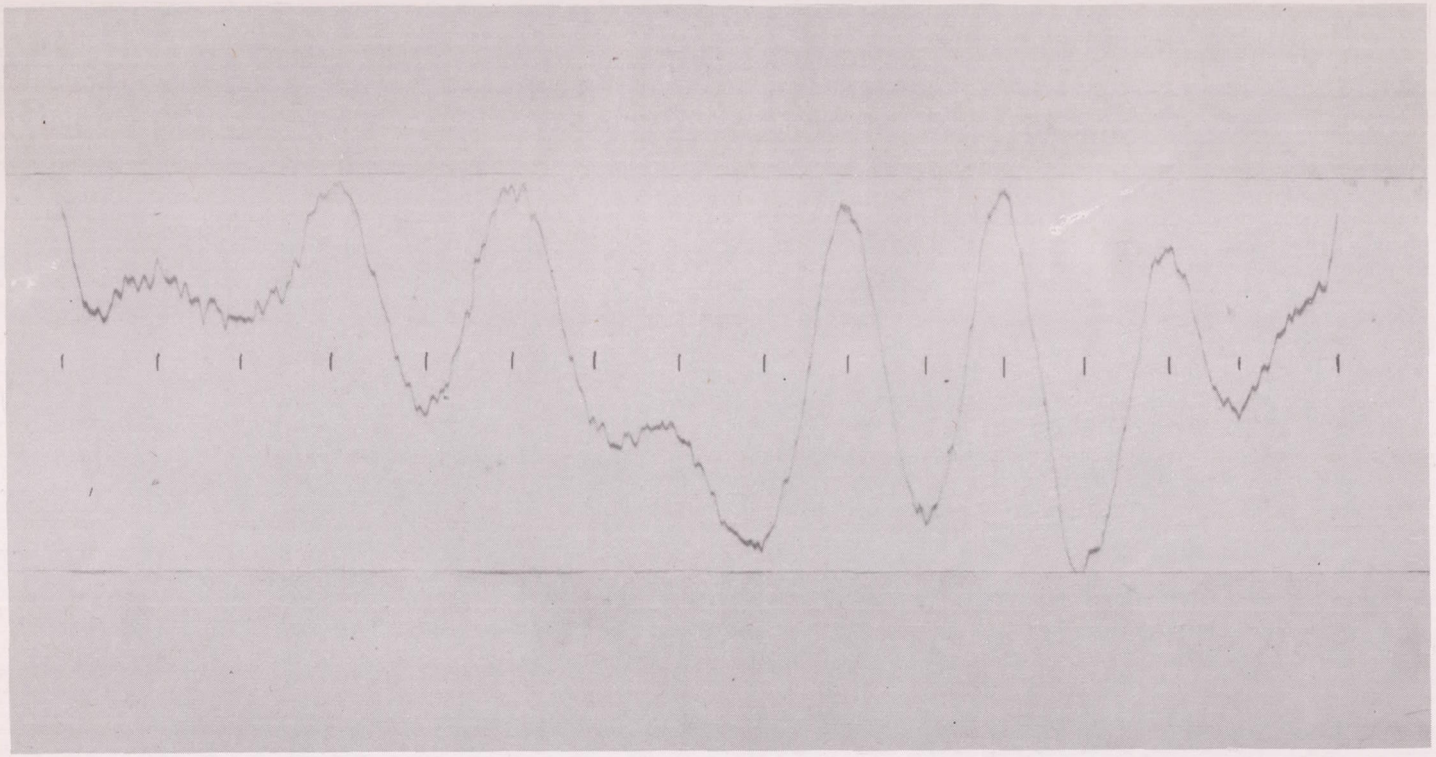

Figure 15.- Photomicrographic trace of the negative of fig. 14, which represents the variations in the density of the image across the uniform portion of the flow. Increasing ordinates represent increasing transmission, that is, dark fringes in the channel.

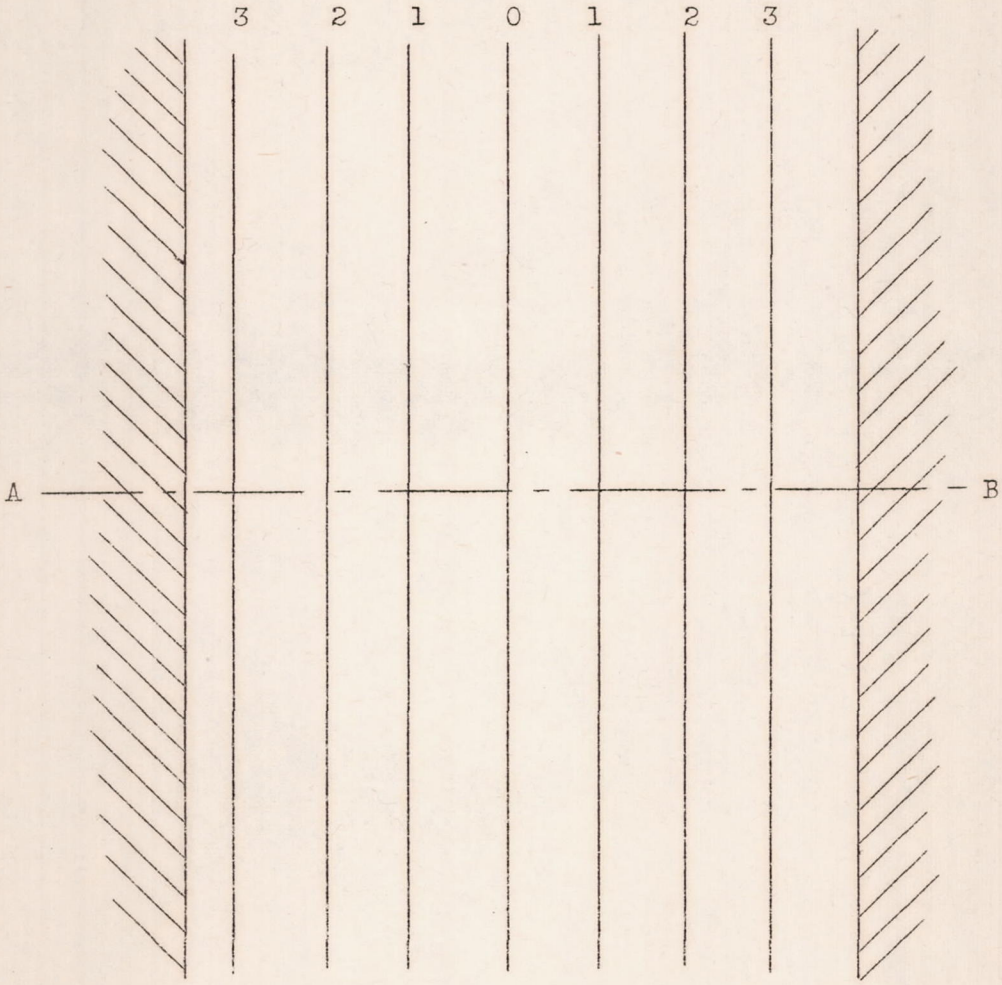

Figure 16.- A tracing of the center lines of the fringes of fig. 14, showing nearly uniform spacing resulting from a parabolic velocity distribution.

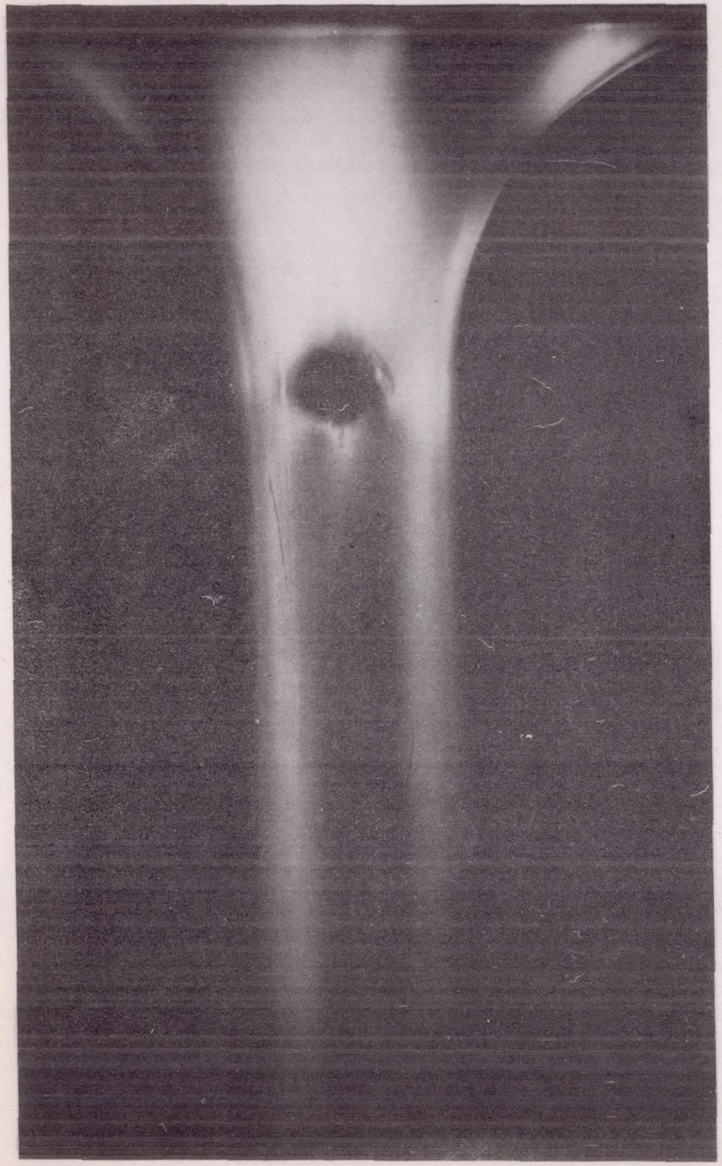

Figure 17.- Fringes in the unobstructed channel taken with plane-polarized light. The polarizer and the analyzer are placed with their axes at 45° to the direction of flow.

Figure 18.- Darkening of half the channel, resulting from placing the polarizer at 33° to the vertical and the analyzer at 33° to the horizontal.

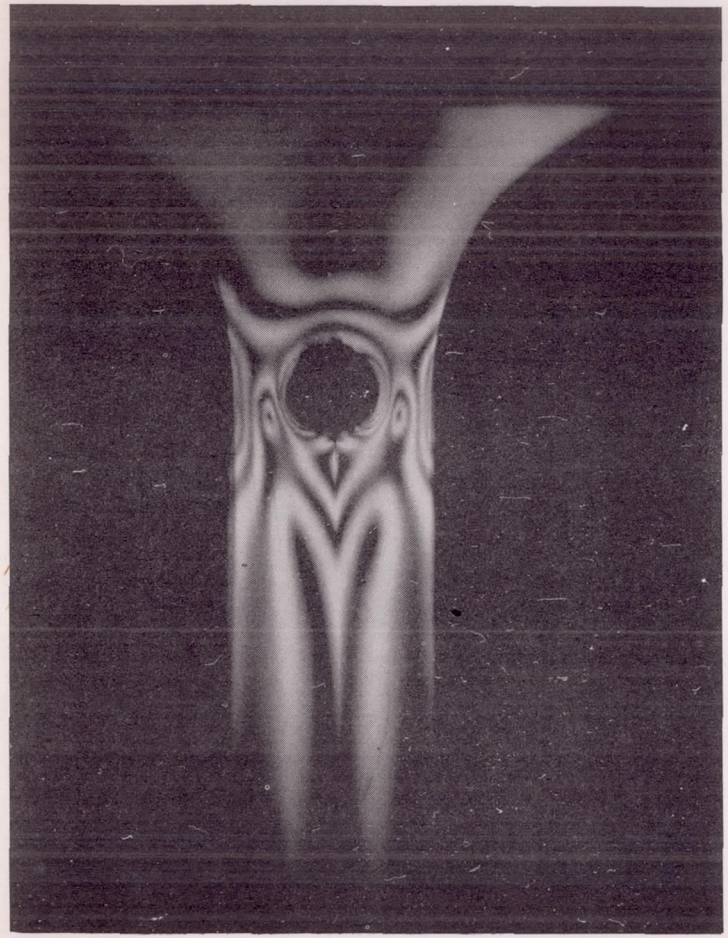

Figure 19.- Fringe pattern resulting from the placing of a cylindrical obstruction in the channel. Discharge rate, 60.5 liters per minute.

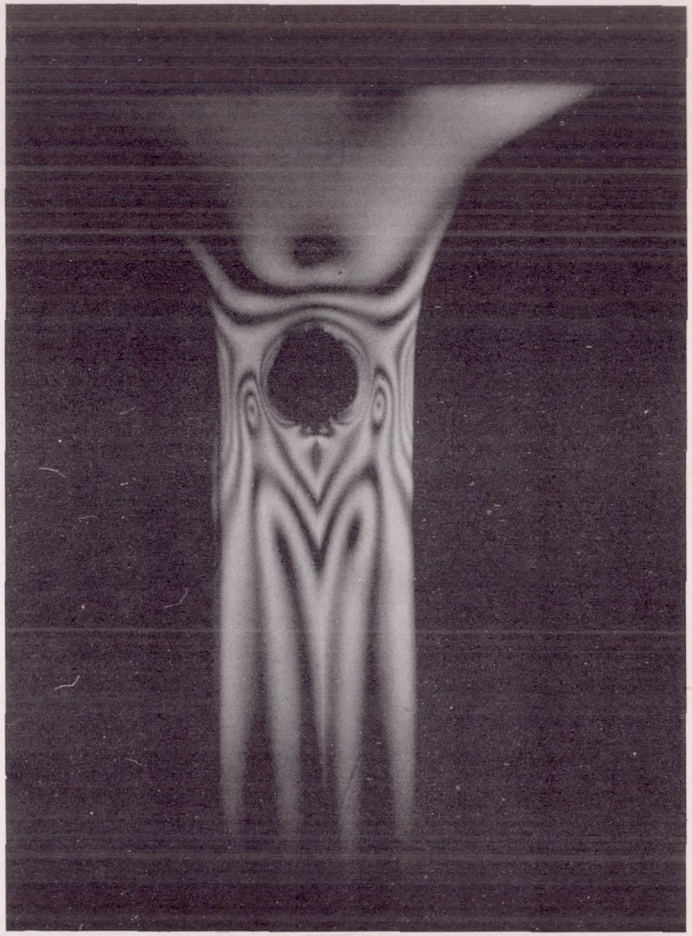

Figure 20.- Fringe pattern resulting from the placing of a cylindrical obstruction in the channel. Discharge rate, 91 liters per minute.

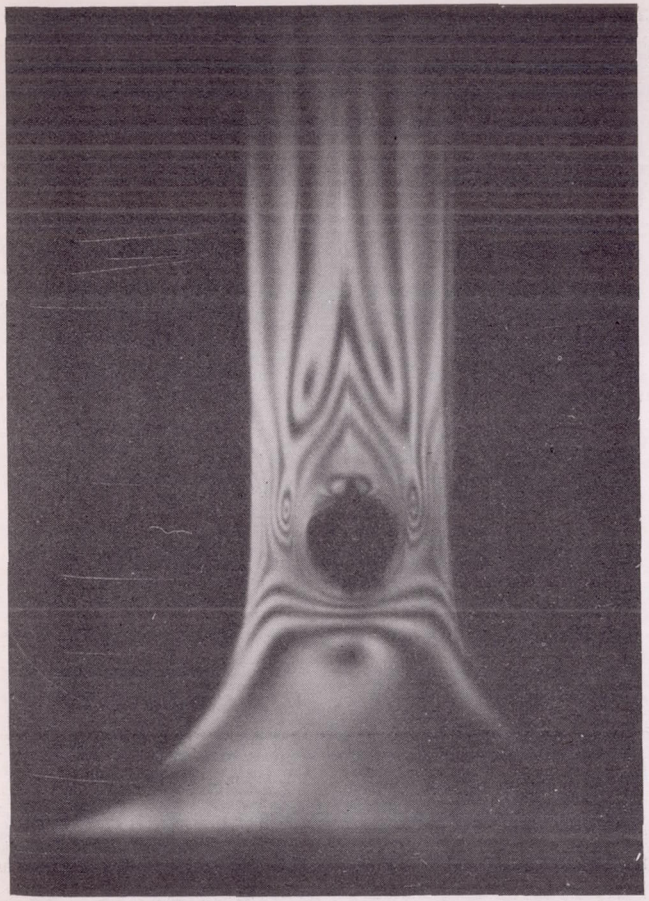

Figure 21.- Fringe pattern resulting from the placing of a cylindrical obstruction in the channel. Discharge rate, 147 liters per minute.

Figure 23.- Fringe pattern due to the streamlined strut section. Discharge rate, 56.7 liters per minute.

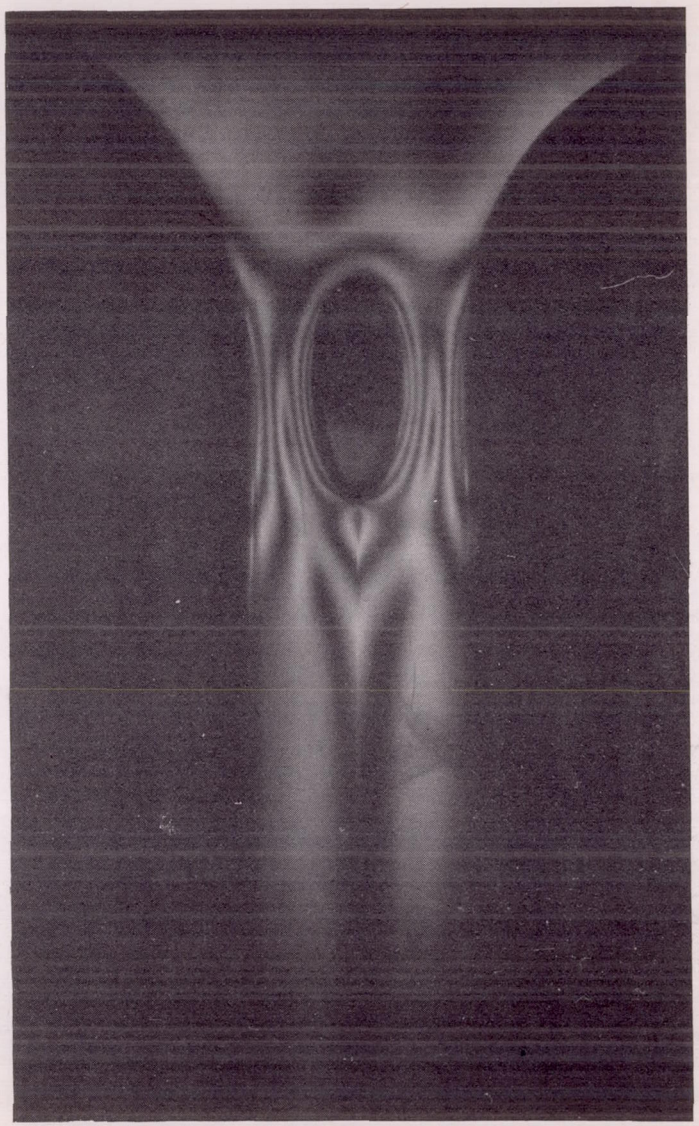

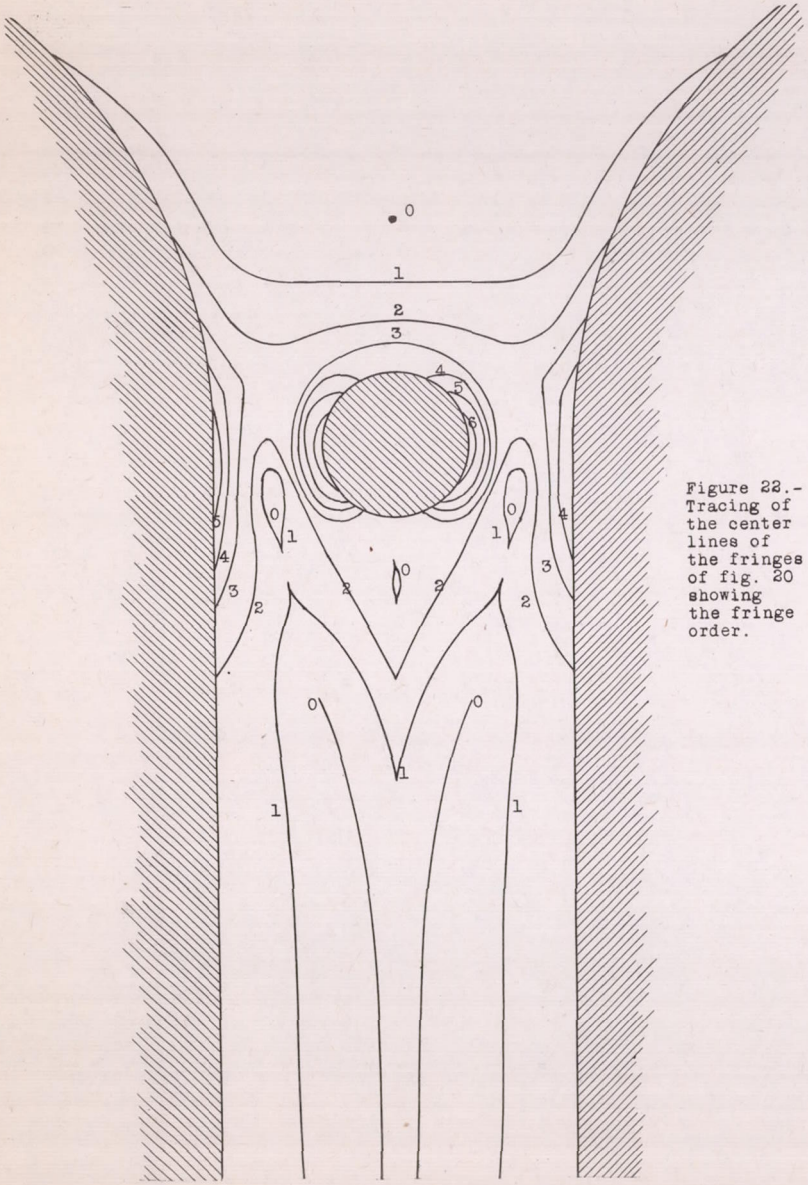

Figure 22.- Tracing of the center lines of the fringes of fig. 20 showing the fringe order.

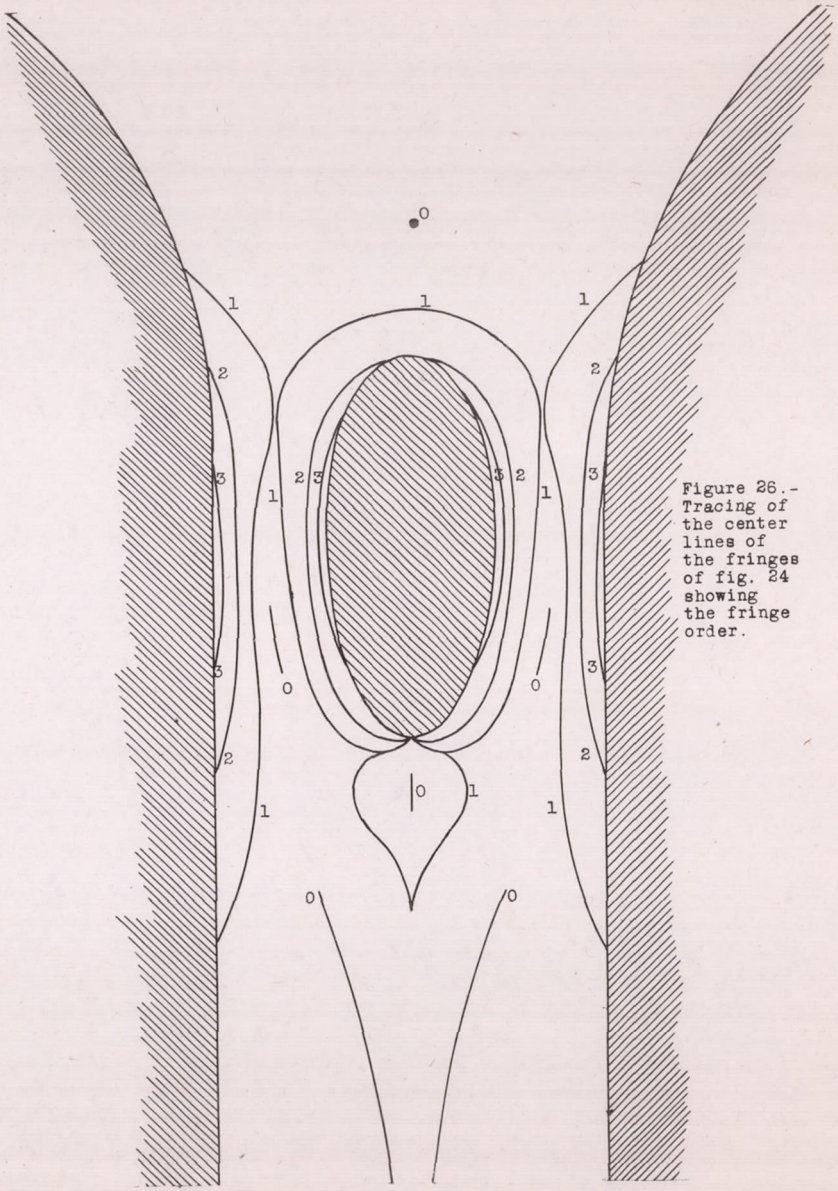

Figure 26.- Tracing of the center lines of the fringes of fig. 24 showing the fringe order.

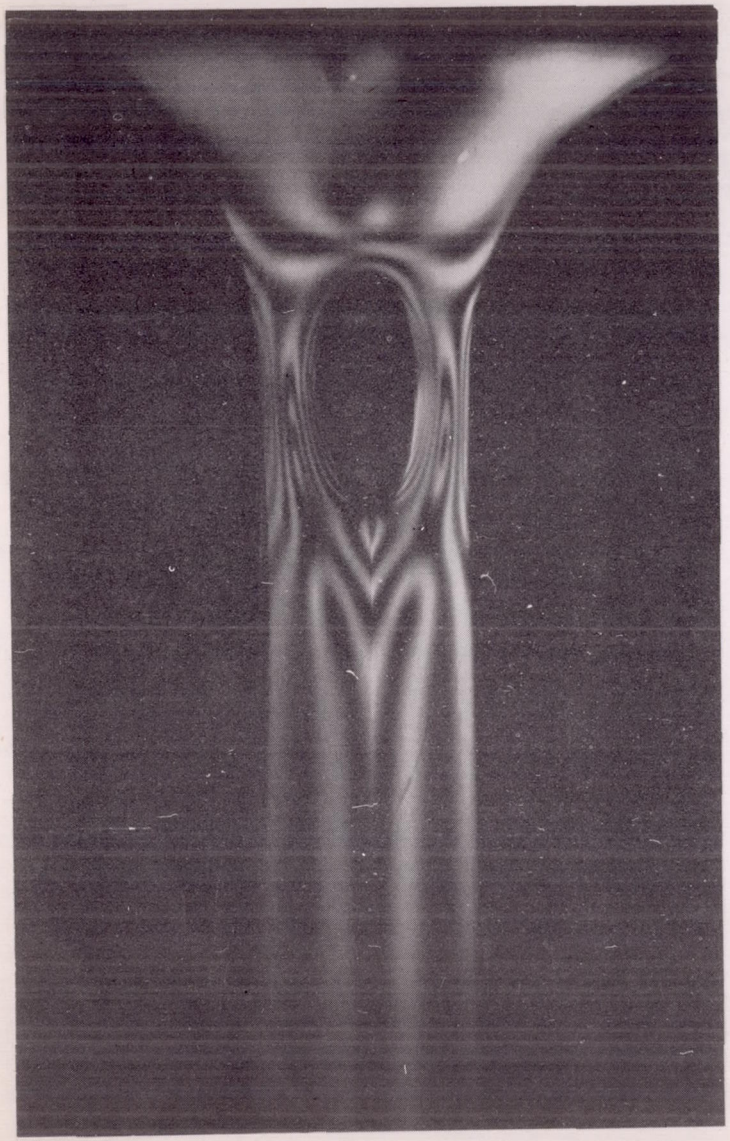

Figure 24.- Fringe pattern due to the streamlined strut section. Discharge rate, 89 liters per minute.

Figure 25.- Fringe pattern due to the streamlined strut section. Discharge rate, 182 liters per minute.

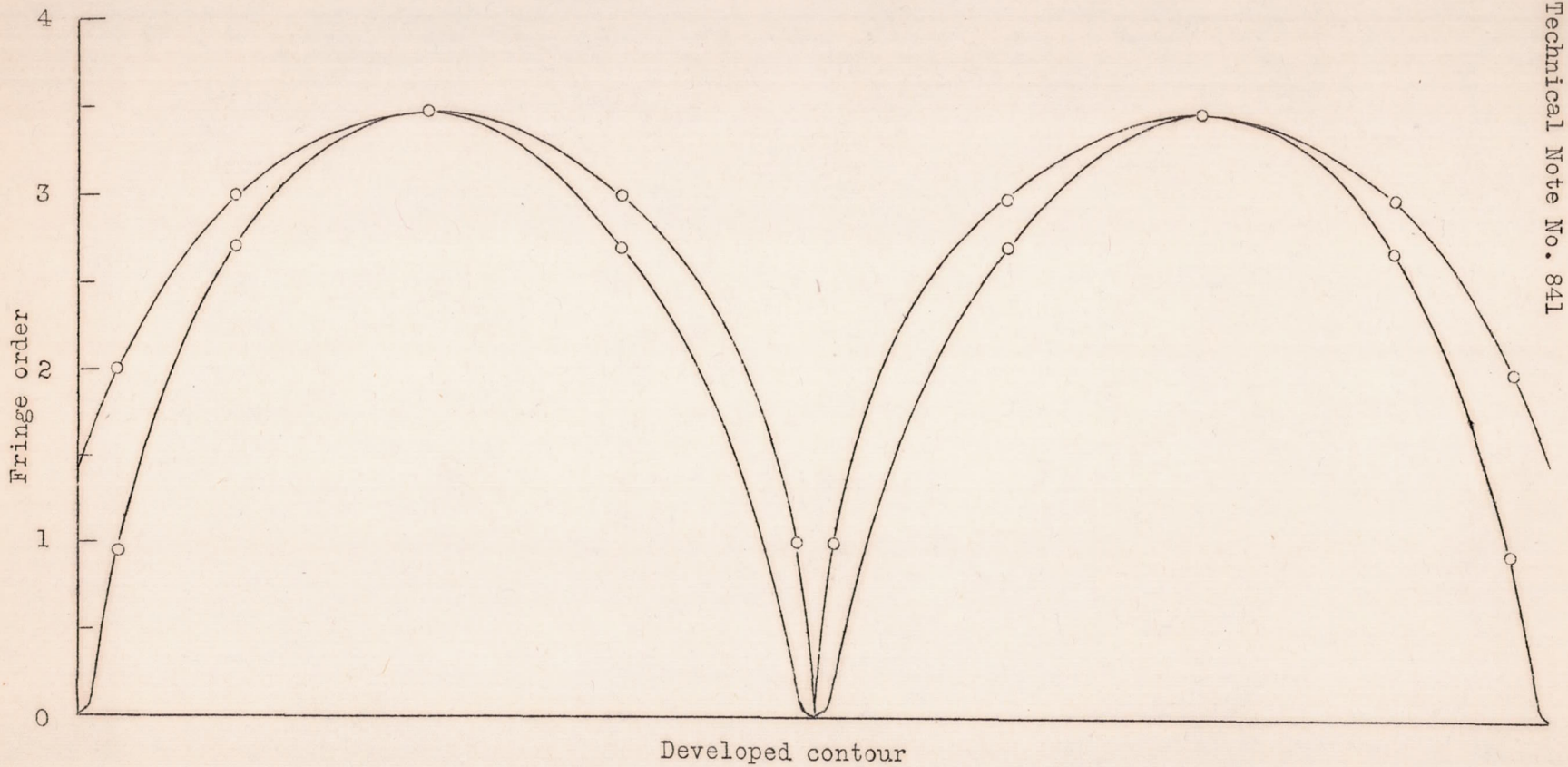

Figure 27.- Development of the boundary of the strut section shown in fig. 23.

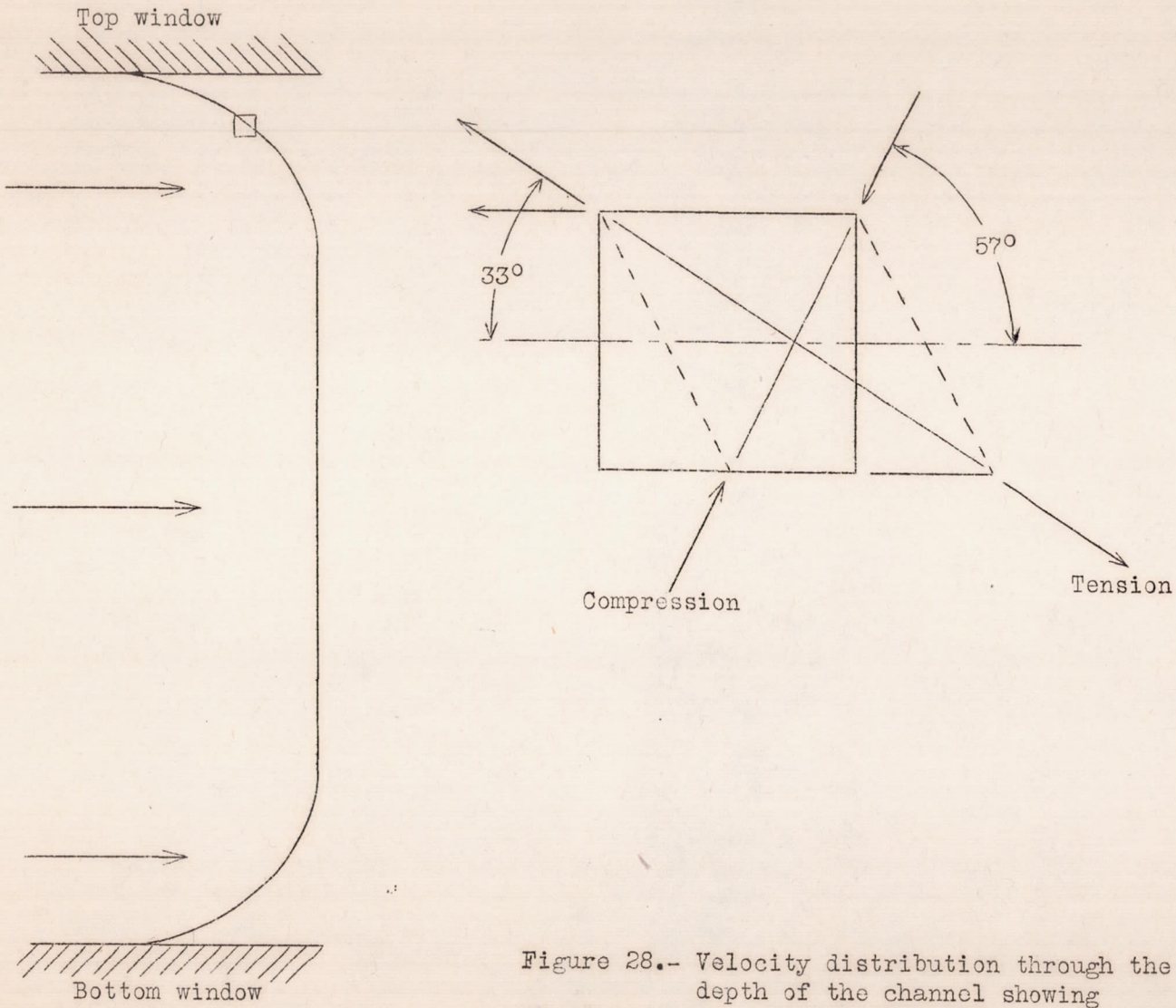

Figure 28.- Velocity distribution through the depth of the channel showing the decrease to zero at the windows.

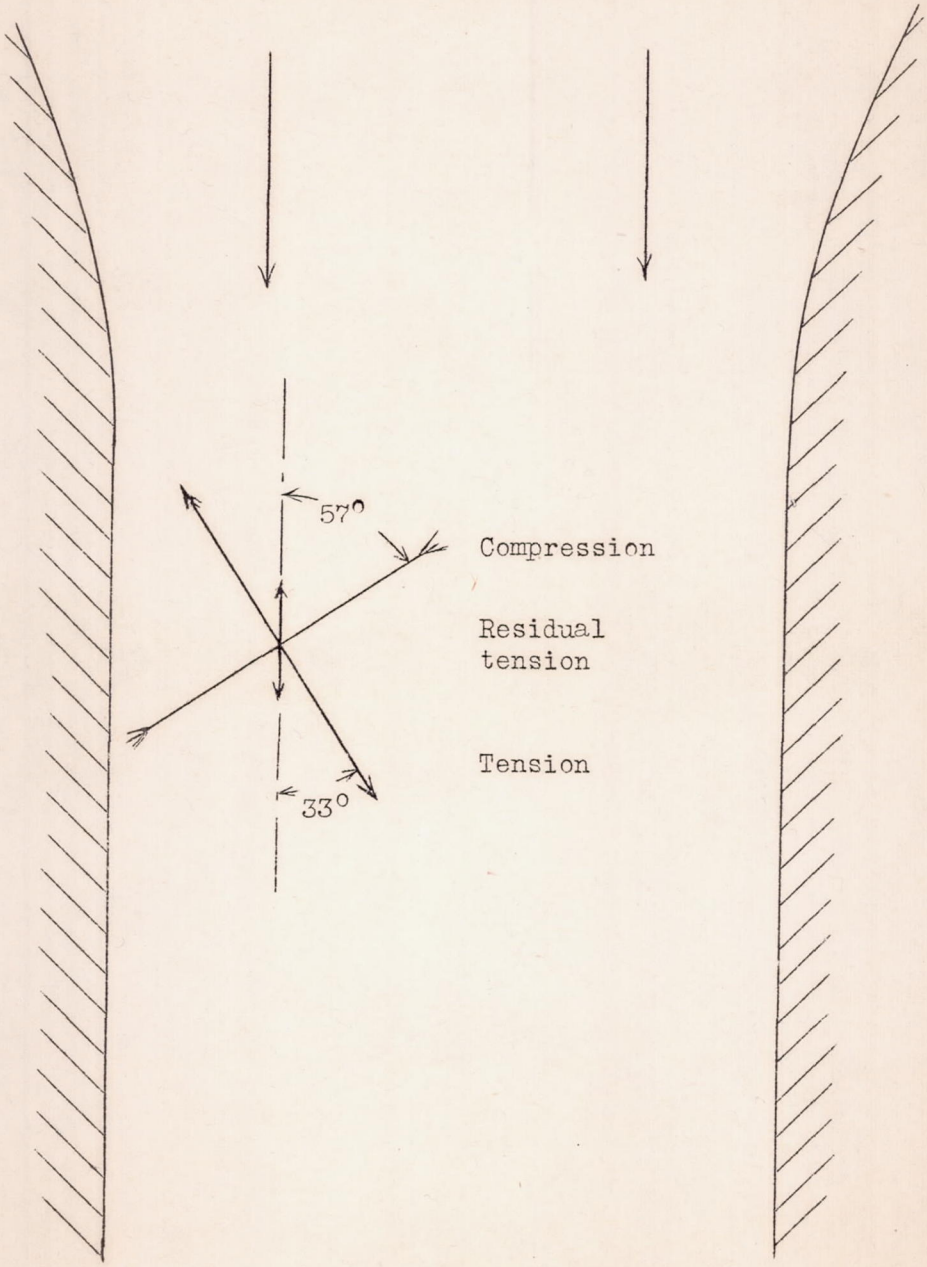

Figure 29.- Sources of double refraction in the channel.